Final Report

MEASUREMENTS IN ATMOSPHERIC ELECTRICITY DESIGNED TO IMPROVE LAUNCH SAFETY DURING THE APOLLO SERIES

By: J. E. NANEVICZ E. T. PIERCE A. L. WHITSON

Prepared for:

NASA MANNED SPACECRAFT CENTER
FACILITY AND LABORATORY SUPPORT BRANCH
HOUSTON, TEXAS 77058
Attention: Mail Code BB321-81

CONTRACT NAS 9-11357

STANFORD RESEARCH INSTITUTE
Menlo Park, California 94025 · U.S.A.

STANFORD RESEARCH INSTITUTE
Menlo Park, California 94025 · U.S.A.

Final Report *June 1972*

MEASUREMENTS IN ATMOSPHERIC ELECTRICITY DESIGNED TO IMPROVE LAUNCH SAFETY DURING THE APOLLO SERIES

By: J. E. NANEVICZ E. T. PIERCE A. L. WHITSON

Prepared for:

NASA MANNED SPACECRAFT CENTER
FACILITY AND LABORATORY SUPPORT BRANCH
HOUSTON, TEXAS 77058
Attention: Mail Code BB321-81

CONTRACT NAS 9-11357

SRI Project 8940

Approved by:

T. MORITA, *Director*
Electromagnetic Sciences Laboratory

RAY L. LEADABRAND, *Executive Director*
Electronics and Radio Sciences Division

Copy No. 8

ABSTRACT

Ground-test measurements were made during the launches of Apollo 13 and 14 in an effort to better define the electrical characteristics of a large launch vehicle. Of particular concern was the effective electrical length of the vehicle and plume since this parameter markedly affects the likelihood of a lightning stroke being triggered by a launch during disturbed weather conditions. Since no instrumentation could be carried aboard the launch vehicle, the experiments were confined to LF radio noise and electrostatic-field measurements on the ground in the vicinity of the launch pad. The philosophy of the experiment and the instrumentation and layout are described.

From the results of the experiment it is concluded that the rocket and exhaust do not produce large-scale shorting of the earth's field out to distances of thousands of feet from the launch pad. There is evidence, however, that the plume does add substantially to the electrical length of the rocket. On this basis, it was recommended that there be no relaxation of launch rules for launches during disturbed weather.

It was found that the exhaust clouds produced during launch are highly charged, and that these charged clouds greatly obscure other electrical effects associated with the launch. Accordingly, it was concluded that further experiments in this general area should include provisions for flight instrumentation.

FOREWORD

The electrical effects accompanying the Apollo 12, 13, and 14 launches are described in this report. Support for the research discussed came from three main sources. For all three launches, most of the data interpretation and theoretical analysis was performed under contractual arrangements with ONR. The experimental work for Apollo 13, were supported by SRI. Contracts from NASA provided funding for the major portion of the Apollo 14 experiments, and for travel and subsistence expenses associated with all three launches.

CONTENTS

ILLUSTRATIONS

ILLUSTRATIONS (Concluded)

TABLES

ACKNOWLEDGMENTS

The authors acknowledge with gratitude the help of many individuals, including coworkers at SRI, who participated in the test program. Others, including NASA personnel, worked behind the scenes to streamline procedures so that instrumentation could be installed and checked out around the pad during the late countdown period when the level of normal activity is very high. In particular we would like to acknowledge the efforts of G. R. Hilbers and W. C. Wadsworth, both of SRI, who worked on fielding and debugging the test instrumentation. Mr. J. E. Mechelay of NASA MSC worked with the experimenters and made certain that all of the last-minute problems associated with fielding an experiment at a new location were expeditiously resolved. Many personnel in Mr. A. J. Carraway's branch at NASA KSC contributed to seeing that the experimenters received the necessary support to assure the success of the program. These included F. Horn, S. S. Perlman, W. Jafferis, and P. D. Toft.

I INTRODUCTION

During the launch of Apollo 12 on 14 November 1969, the launch area was covered with a cloud layer that did not exhibit any thunderstorm activity, but that contained high electric fields. These weather conditions (no active storm cells within the clouds and no lightning in the vicinity of the launch area) fell within the permissible conditions for a launch under the existing launch rules. Accordingly the vehicle was launched into the clouds. Thirty-six and one-half seconds after launch, when the vehicle reached an altitude of 6,400 feet it was struck by lightning, causing a current overload circuit to function and disconnecting ship's prime power.[1]* Another strike to the vehicle occurred 52 seconds after launch when it reached an altitude of 14,000 feet.

Following the Apollo 12 lightning incident the available data were analyzed, and it was concluded that although there was no lightning activity in the cloud at the time of launch, high electric fields did exist, and the rapid introduction of the Apollo vehicle (and its exhaust plume) into this high field region triggered the strokes. Indeed, it is likely that had the vehicle not been introduced into the clouds, no strokes would have occurred. When the cause for the Apollo 12 lightning incident was established, the launch rules were modified to prevent launches into clouds of the type likely to contain high electric fields.

---

* References are listed at the end of the report.

NASA recognized that certain aspects of the Apollo lightning triggering problem were poorly understood and invited scientists specializing in the study of lightning and atmospheric electricity to propose experiments to be performed in connection with future launches in an effort to gain further insight into the general problem. In particular, the experiments were directed at ensuring that future launch rules would be satisfactory from the standpoint of both safety and the avoidance of unnecessary delays. Since Apollo 13 was scheduled to be launched on 11 April 1970, there was no possibility of conducting on-board measurements on this vehicle. Furthermore, the time and funding limitations for participation in the Apollo 13 launch dictated that only existing instrumentation capable of being packaged to work in the field could be considered for the experiments.

In considering the Apollo lightning triggering problem in general, it was evident that little was known of the electrical character of large rockets in flight. For example, it was agreed that the electrical conductivity of the plume would make the rocket appear electrically longer than its actual physical length, but the amount of the increase in length was uncertain. Establishing bounds on this length was important since it markedly affects the likelihood of a stroke being triggered in a given ambient electric field. Obviously, if the combination of rocket and plume looks like a very extended conductor such as the Empire State Building the launch rules should be more stringent than if the plume merely doubles the length of the rocket.

It should be mentioned that a preliminary survey[2] of triggered lightning incidents, initiated shortly before the Apollo 12 occurrence, suggested that most such incidents satisfy two common criteria: (1) the general ambient electric field is of the order of 10 kV/m, and (2) the potential discontinuity between the conductor initiating the lightning and the adjacent atmosphere approaches 10^6 V. A more thorough study[3]

has confirmed this impression. This potential discontinuity will of course be greater if either the ambient field or the effective electric length of the conductor increase. To all appearances, these conditions (ambient field of 10 kV/m and potential discontinuity of 10^6 V) were certainly approximated during the Apollo 12 incident.

It was also observed during the consideration of the Apollo 12 incident that little was known regarding the static electrification of rockets after launch. Airplane experience indicated that engine charging raised the potential of the aircraft to hundreds of kilovolts as soon as the wheels left the ground. Experience with Nike Cajun rockets indicated that they too became charged by the action of the rocket motors, but it was felt that extrapolating data from a 12-inch- or a 6-inch-diameter solid-fuel rocket motor running for 3 seconds to a 30-ft-diameter liquid-fueled rocket burning for almost three minutes would be of doubtful merit. A high potential on the rocket would alter the magnitudes of the electric fields in its vicinity and could affect the likelihood of a stroke triggered by the rocket. There is some evidence that this effect does occur for aircraft.[3] Accordingly, it was felt that information regarding in-flight rocket potential would be of considerable significance.

This report concerns experiments, carried out during the launches of Apollo 13 and Apollo 14, and directed at investigating some of the points discussed above. The report considers material already presented in preliminary reports[4,5] in much greater detail; it also contains considerable supplemental information and additional analysis.

II DESCRIPTION OF EXPERIMENT AND INSTRUMENTATION

A. General

The limitations on time and funding discussed in Section I dictated that the experiment, on the Apollo 13 launch at least, must be conducted using existing instrumentation. The restriction that the experiment be confined strictly to ground-based measurements further circumscribed the possible alternatives available.

With these limitations in mind, it was observed that existing ground-based instrumentation was capable of providing considerable information regarding the electrical character of the vehicle after launch. The arguments proceed with the aid of Figure 1. In fair weather, there is at the surface of the earth a static electric field normally of 100 to 300 volts per meter; the magnitude depends mostly on the degree of atmospheric pollution. This fair-weather field is shown as the ambient field in Figure 1. If a large grounded body such as a rocket on a pad is placed in this field as illustrated in Figure 1(a), the field intensity on the ground in the vicinity of the rocket will be reduced below the ambient as shown in Curve a of Figure 1(f). If the rocket is now raised above the ground as shown in Figure 1(b), the field intensity in the vicinity of the pad will be given by Curve b. Here we observe that there is an enhancement of field in the immediate vicinity of the pad. If the size of the rocket is augmented by a conducting plume as in Figure 1(c), the field enhancement will be more pronounced and will extend over a wide region as shown in Curve c. If, on the other hand, the exhaust is highly conducting for many rocket lengths, the field will be reduced below the ambient value for a distance of the order of the

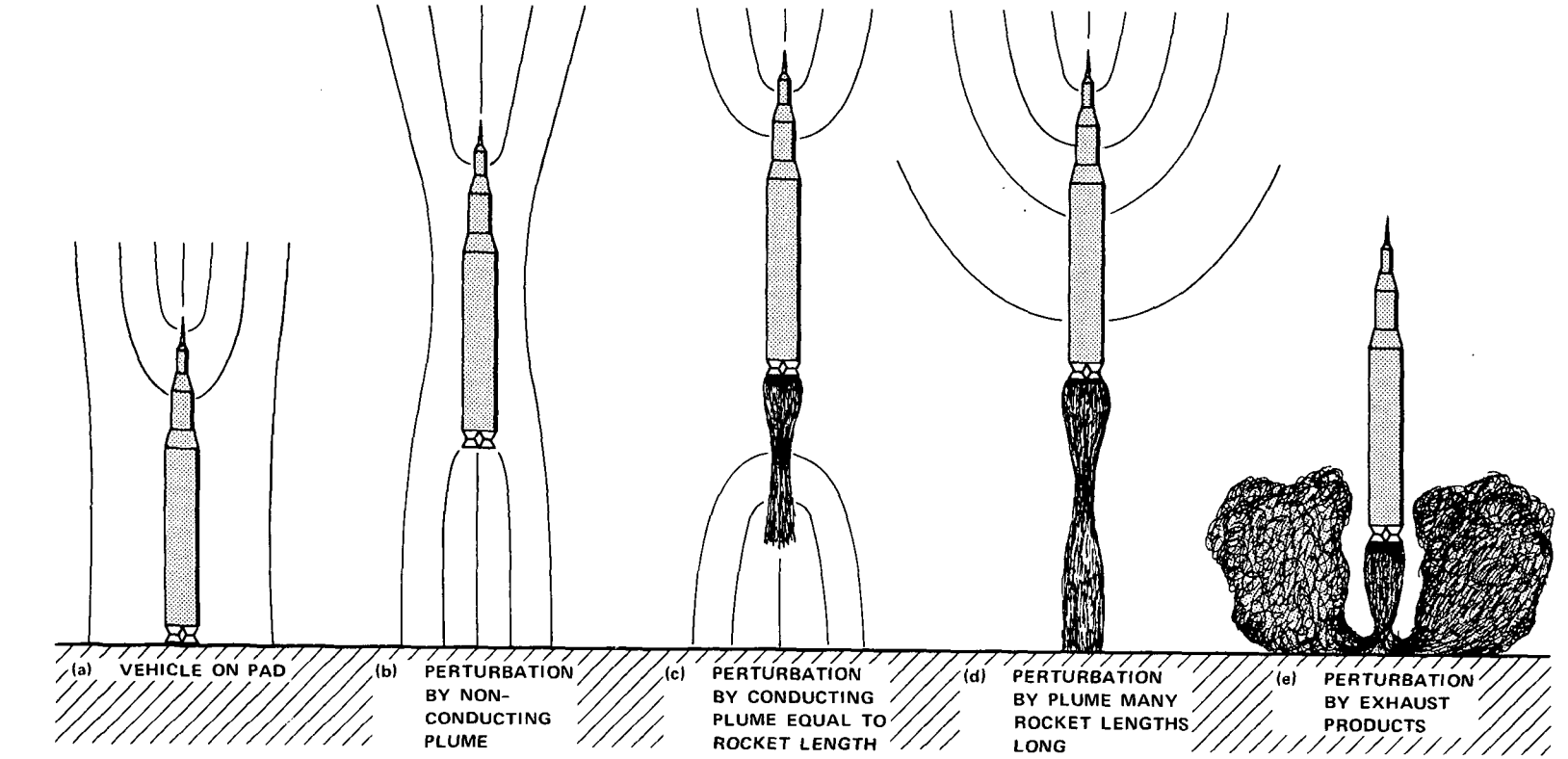

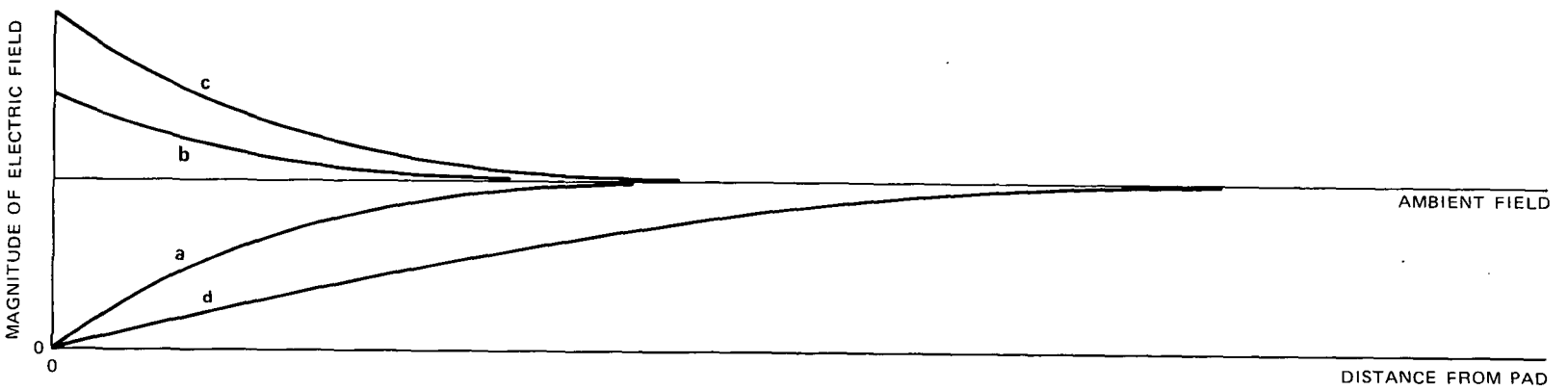

TA-8940-1

FIGURE 1 POSSIBLE PERTURBATIONS OF EARTH'S FIELD CAUSED BY ROCKET LAUNCH

conducting plume length as suggested in Curve d. Finally, it is possible that the exhaust products, debris stirred up by the launch, and clouds due to the interaction between the exhaust and the cooling water, as shown in Figure 1(e), are highly charged, and that the electric fields in the vicinity of the pad are governed largely by these charges.

The above arguments indicate that measurements of static electric field in the vicinity of the launch pad prior to and during launch can provide considerable insight into the electrical length of the rocket plume. Since field meters capable of detecting the earth's field in fair weather existed at SRI, and were available for use in an outdoor environment, it was decided that they would constitute a major portion of the SRI instrumentation for the Apollo 13 experiment.

Experience with aircraft[6,7] and small rockets[8] indicated that the engine exhaust generally is not completely neutral, so that it carries charge away from the vehicle, charging the vehicle to a high potential as illustrated schematically in Figure 2. As the potential continues to rise, the electric fields at the extremities finally become so high that dielectric breakdown of the air and corona discharge occur to relieve some of the charge.

It should be emphasized that even after the corona threshold occurs, the potential of the vehicle will continue to rise quite considerably, until--in the absence of other current mechanisms--the engine-charging and the corona-discharging currents balance.[9] Typically, with an aircraft equipped with static dischargers the corona onset will be at a potential of some 20 kV, but the balance between engine and corona currents will not be attained until the potential is perhaps 100 kV.[6] The corona breakdowns generate RF noise that can be detected with the proper receiving equipment either on the rocket or on the ground. The character of the noise pulses is such that the equivalent noise fields

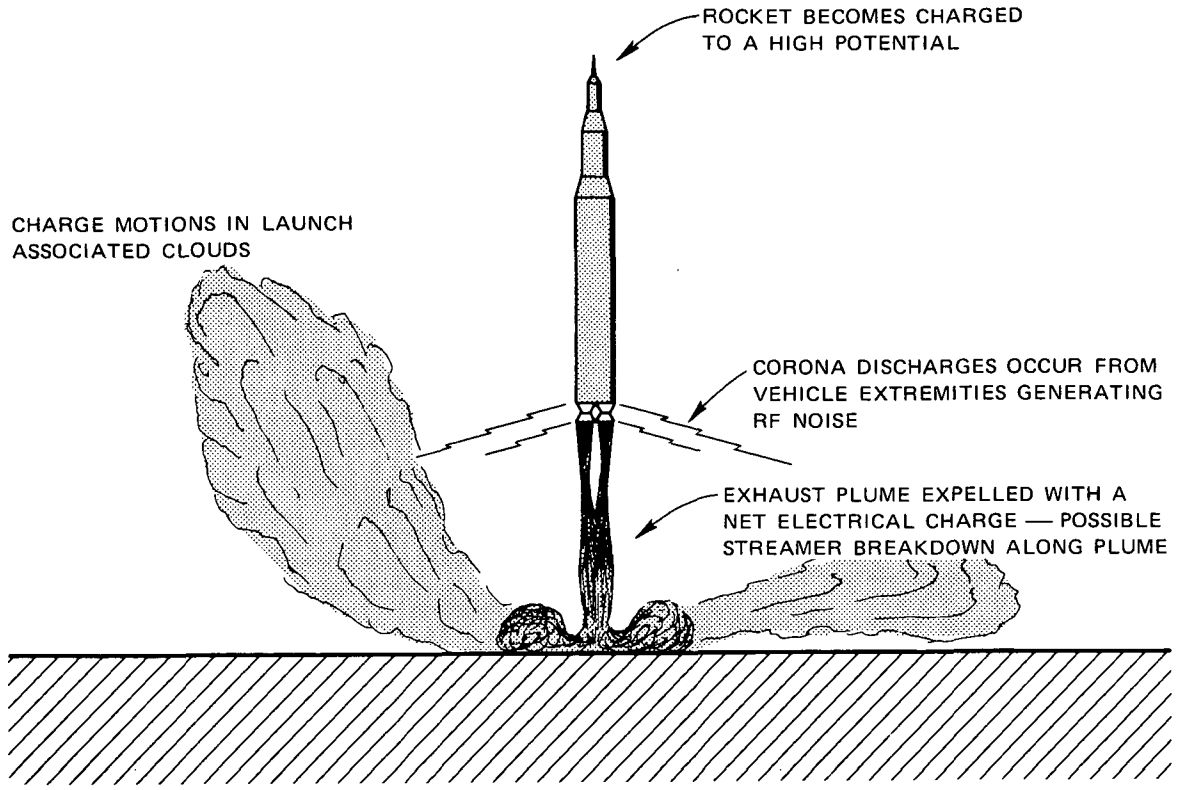

FIGURE 2 POSSIBLE RF NOISE GENERATION AS THE RESULT OF ROCKET-MOTOR CHARGING

are highest at low frequencies. Corona processes are not the only possible generators of radio noise associated with the rocket environment. Spasmodic streamer breakdown along the exhaust plume, of which there is evidence from film records, would be expected to produce noise. Also, radio noise will inevitably be generated by the acceleration of charges whether these are moved macroscopically on the vehicle, exhaust plume, and exhaust-associated clouds, or are churned locally by turbulent eddies.

To carry out LF noise measurements on an earlier program, SRI had assembled a set of five narrowband receivers covering the frequency range 1.5 to 120 kHz. These receivers were not in current use and could be fielded in short time. Accordingly, it was decided that the Apollo 13 instrumentation should include these receivers to measure LF RF noise in

an effort to obtain some indication whether the vehicle potential became sufficiently high during launch to cause electrical discharge from the extremities.

B. Instrumentation

In planning the ground field-meter layout for Apollo 13, the objective was to site the instruments so that one could determine which of the options of Figure 1 best satisfied the measured results. In order to measure ambient-field diminution of the sort caused by a short plume, or a field enhancement of the sort illustrated in Figure 1(b), it is necessary to place one field meter as close as possible to the pad. Additional field meters are then located at points successively farther away from the pad until one either runs out of field meters or is convinced that he has reached the limit of the detectable perturbation.

In planning the SRI field-meter installation, it was observed that the rocket exhaust from the Apollo vehicles is not simply allowed to fall on the pad and be deflected symmetrically. Instead, the exhaust is channeled into two flame trenches; one extending to the north of the pad, and the other to the south of the pad as shown in Figure 3. To minimize possible perturbations from the exhaust products, it was decided that the main array of three field meters would be located along a line west of the pad roughly at right angles to the flame trenches. (Marshy land around the pad prevented installation of instrumentation along a line precisely at right angles to the trench line.) Field meters were installed at the following stations:

- Camera Pad 5, 400 m from pad
- Slide-wire area, 850 m from pad
- Crawlerway, 1750 m from pad.

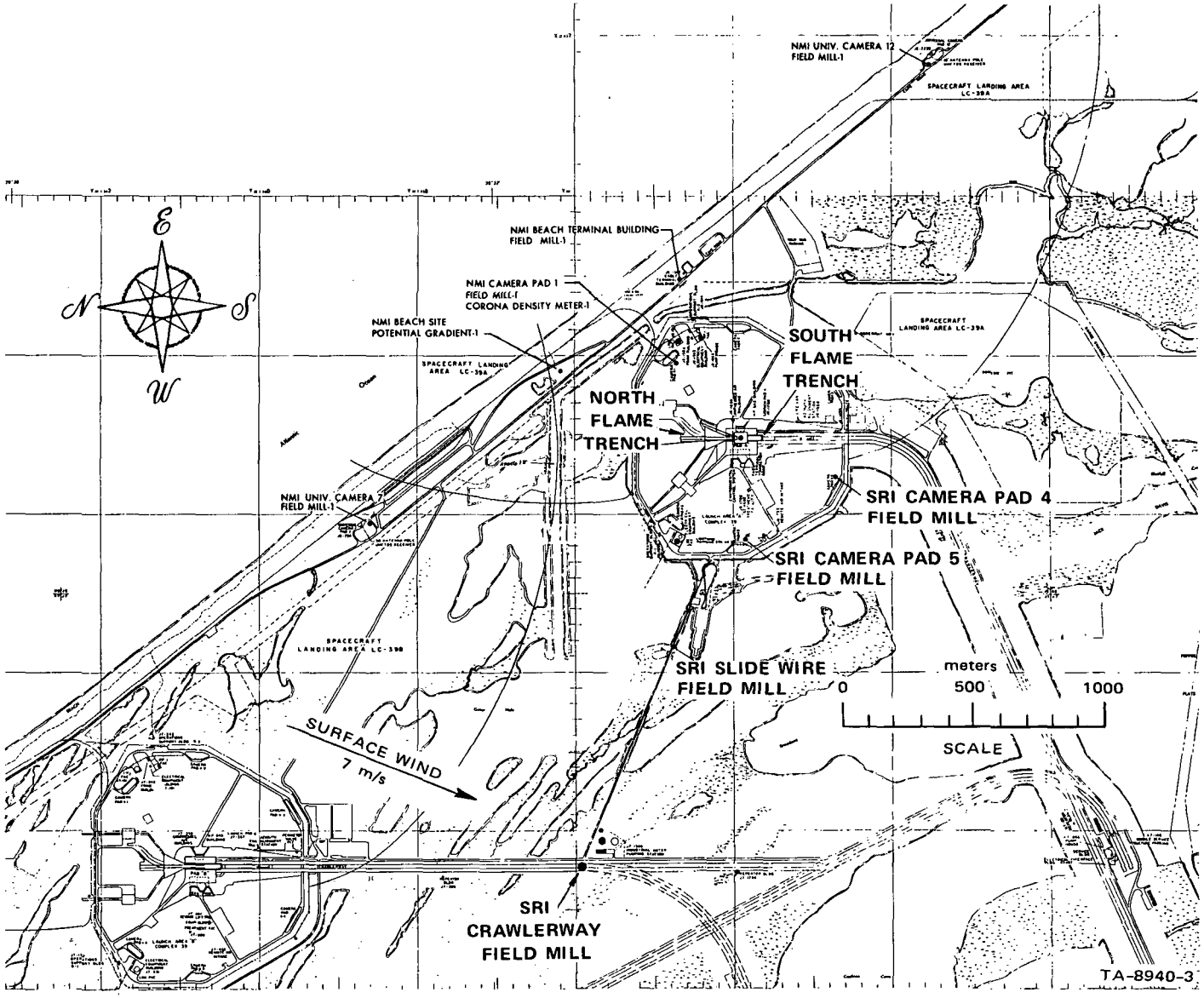

FIGURE 3 INSTRUMENTATION FOR APOLLO 13 LAUNCH

To investigate the effect of charge in the exhaust in producing field perturbations, it was felt that one field meter should be positioned to couple strongly to the rocket exhaust. Accordingly, one field meter was located in the vicinity of Camera Pad 4, as close to the south flame trench as considered prudent. It should be noted at this time that the north flame trench is flat, so that its flame moves horizontally away from the rocket. The south flame trench has a ramp approximately 50 m from the rocket to direct the south flame upward. Thus, during the early stages of the launch, the south flame trench exhaust products passed nearly over the Camera Pad 4 field meter.

Since more than one organization was carrying out measurements, it was important that an effort be made to provide points at which measurements could be compared and yet not allow undue duplication of measurements. To achieve this, the New Mexico Institute of Mining and Technology[10] installed field meters on the opposite side of the pad, as shown in Figure 3, and, in addition, had field-meter installations at various stations along the beach. The most distant of these was 700 m north-northwest of the pad, in order to permit the detection of a large-scale field perturbation such as that illustrated in Figure 1(d).

Instrumentation for the LF noise experiment was installed at Camera Pad 5. The arguments for this choice were that the receiving antenna should be as close as possible to the vehicle to maximize coupling to corona discharges, sparking, or other noise-generating mechanisms associated with liftoff. On the other hand, it was important that the instrumentation not be placed so near the pad that acoustic noise during the launch might affect its operation. A final practical consideration was that 110-V, 60-Hz power had to be available for the receivers and recorders. Camera Pad 5 met all of these requirements.

For the launch of Apollo 14, the instrumentation was expanded as shown in Figure 4. The SRI instrumentation system retained the array of field meters along a line roughly west of the pad and the mill at Camera Pad 4. The crawlerway field mill was moved slightly south along the crawlerway road to place it due west of the pad. To gain a better idea of the character and extent of the south exhaust plume, an additional field mill was installed at the southern boundary of the parking lot south of the pad.

The main new measurement concept added for the Apollo 14 launch was the use of a field meter on the face of the launch umbilical tower (LUT) at the 340-ft level facing the rocket. The results for Apollo 13 had strongly suggested that the clouds generated by the exhaust and its interaction with the cooling water were substantially charged. Since these clouds were closer to the field-meter network used for Apollo 13 than was the vehicle, the electrical effects of the clouds tended to mask any changes due to charge on the vehicle. In order to identify conclusively the relative cloud and rocket effects it was necessary to install a field meter where it would be influenced essentially only by the rocket charge. The launch umbilical tower was a suitable place. It was argued that a field meter at this location would couple strongly to the launch vehicle as it passed, and would provide a good indication of vehicle potential at least until the vehicle cleared the pad.

The individual pieces of instrumentation were improved and adjusted as considered appropriate on the basis of Apollo 13 experience. Aside from the addition of the LUT field meter, no major changes in experiment concept were made for Apollo 14.

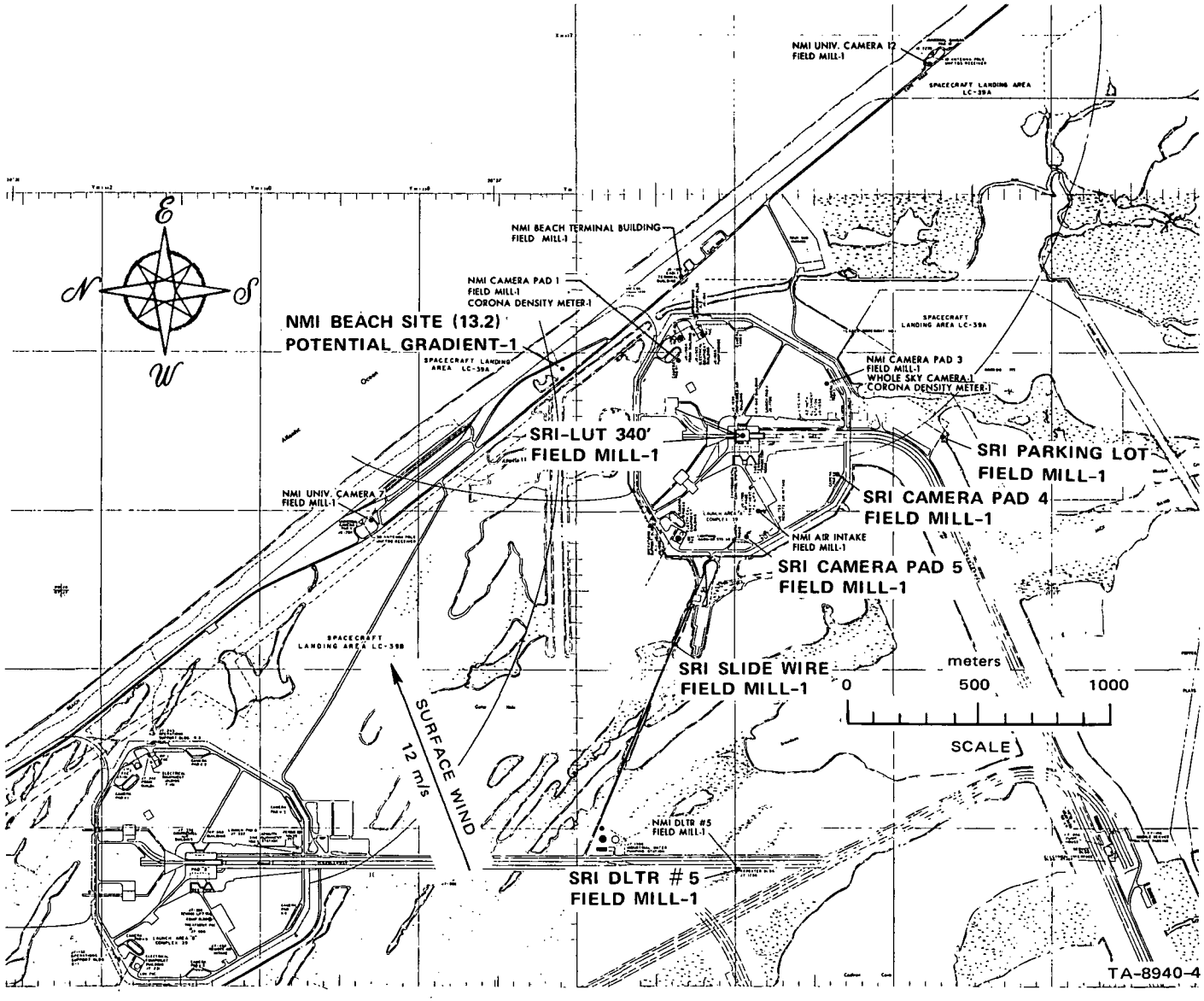

FIGURE 4 INSTRUMENTATION FOR APOLLO 14 LAUNCH

A photograph of a typical ground field-meter installation is shown in Figure 5. All of the electronics and the strip-chart recorder were housed in a plywood box that protected the system from the weather and provided a convenient base for sandbagging to protect the instrumentation from the launch blast. (This arrangement proved to be very satisfactory in that there was no damage to any of the systems after any launch.) The top of the box was covered with a sheet of aluminum that provided a well-defined ground plane for the field-meter detector head. A box of the sort used for the field-meter installation produces a localized perturbation of the ambient electrostatic field with the result that the magnitude of the field at the field-meter detector-head location is higher than the ambient field. Model measurements in the laboratory indicated that, for the form of the boxes and sandbagging used in the Apollo experiments, the field augmentation was 1.6. (In reducing the data from the Apollo experiments the measured field value was divided by 1.6, so that the results are presented in terms of actual ambient field.)

Figure 5 is also of interest in that it provides perspective on the siting of the Camera Pad 4 installation. The south flame is directed upward by the flame trench so that it comes out at the south end of the mobile service structure (which is moved away for the launch). Thus this meter should respond strongly to charge carried away in this portion of the exhaust.

All of the field-meter sites were chosen to have the general character of the installation illustrated in Figure 5. The field meters were installed on flat ground, far from buildings, poles, wires, and other objects that might cause field perturbations.

The position of the Camera Pad 5 site with respect to the launch vehicle is shown in Figure 6. Here again, the terrain is flat, and

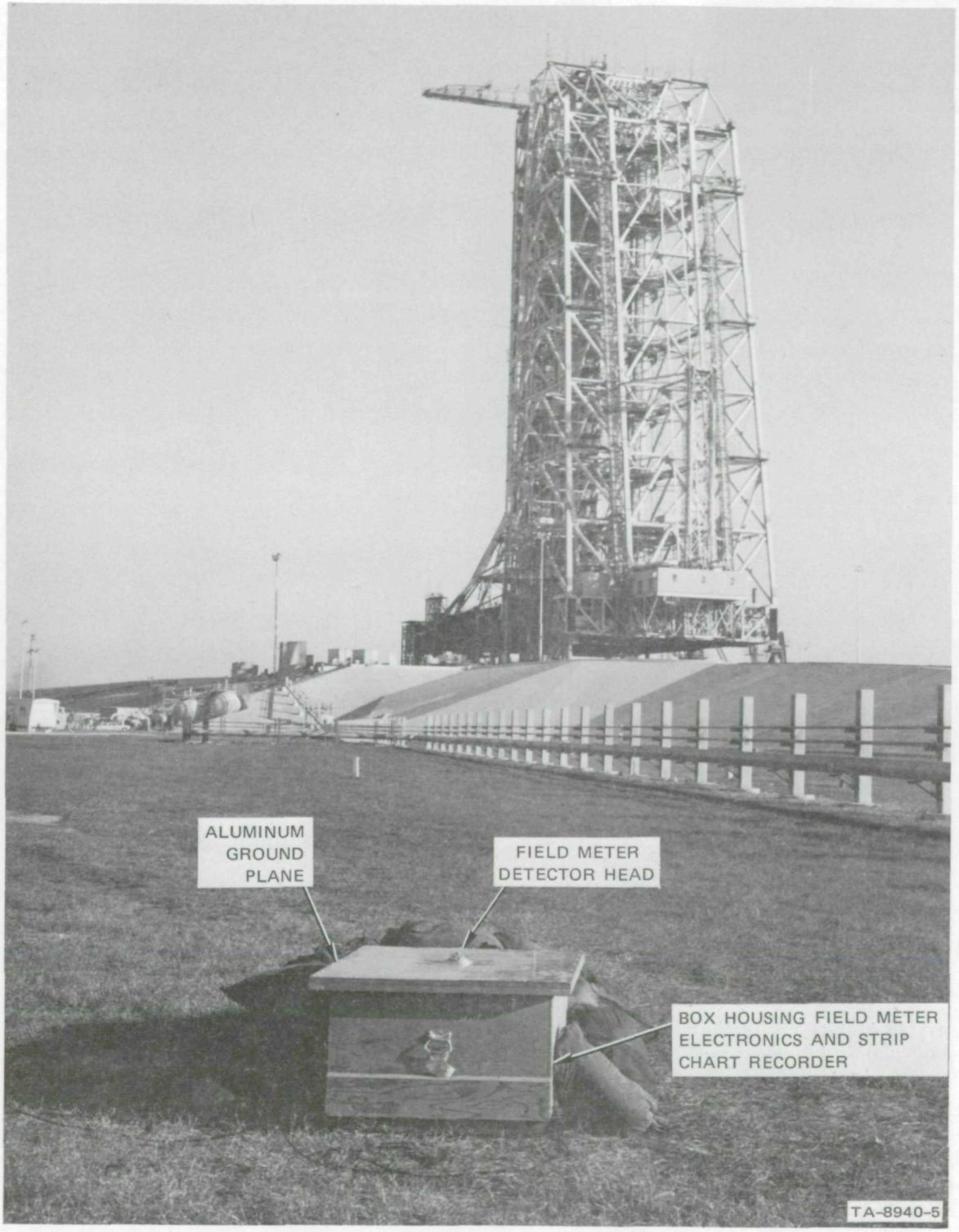

FIGURE 5 TYPICAL FIELD-METER INSTALLATION — CAMERA PAD 4, APOLLO 14

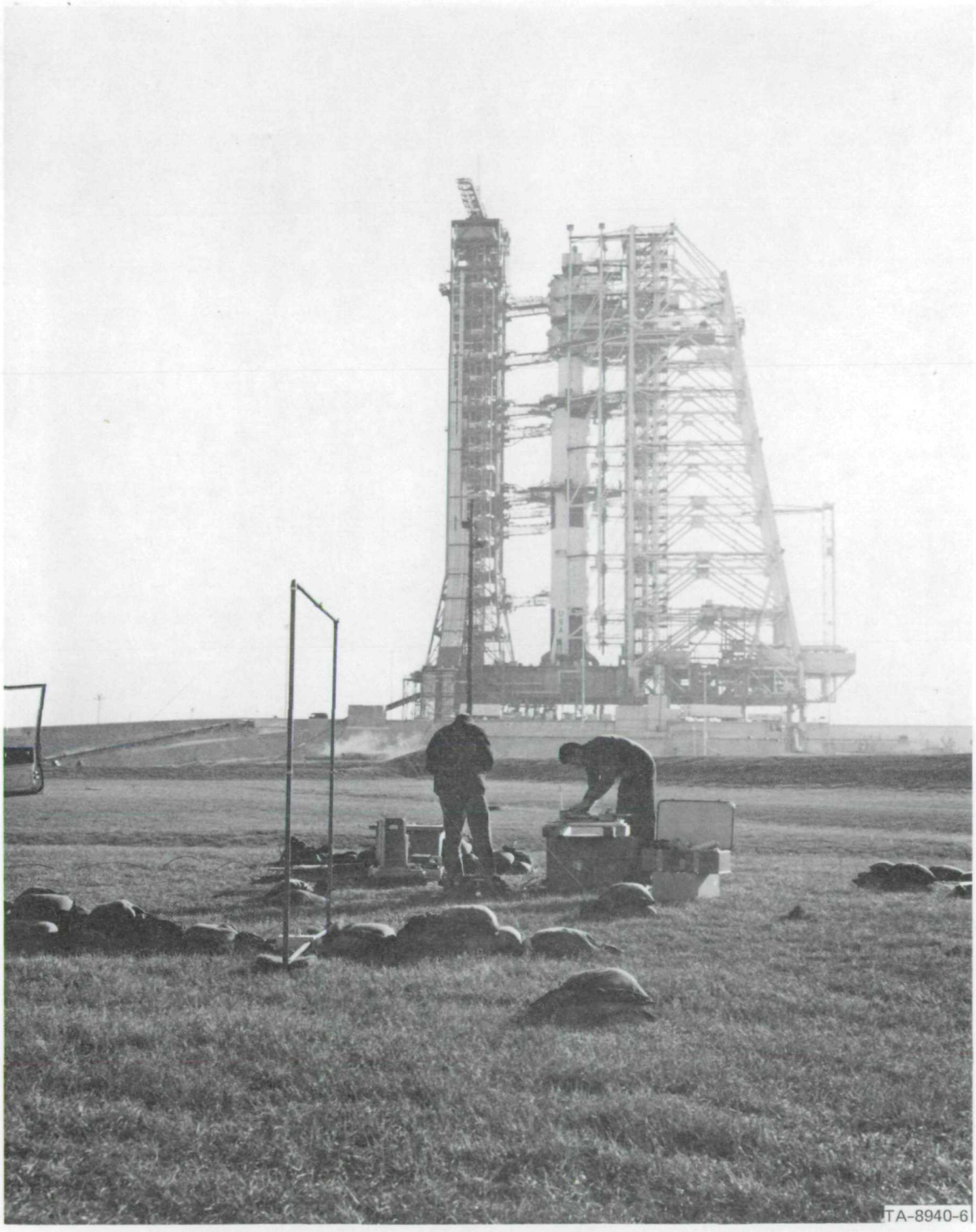

FIGURE 6 CAMERA PAD 5 INSTRUMENTATION FOR APOLLO 14, SHOWING POSITION WITH RESPECT TO PAD

there are no structures in the immediate vicinity to produce perturbations of the ambient field. This site is at right angles to the flame trench in order that the fields be influenced to the least extent by charged particles in the exhaust products. Also evident in the figure is the arrangement of the loop receiving antenna. The antenna was oriented so that the Apollo rocket fell in the plane of the loop to maximize coupling between the loop and possible noise sources on the rocket. Preamplifier electronics associated with the loop antenna were mounted in a cast aluminum box located in the middle of the bottom leg of the loop. An accelerometer to measure mechanical vibration was attached to this same cast aluminum box.

Additional details of the Camera Pad 5 installation for the launch of Apollo 14 are shown in Figure 7. The plywood box housing the field-meter sensor was located in the middle of a flat, clear region. Field-meter electronics and the LF noise receivers were housed in this box, which was sandbagged to protect it from the launch blast. The tape recorder and strip-chart recorder (not shown in the figure) were located in a line behind the field-meter box for shielding from the blast. The electric dipole antenna used on Apollo 14 was mounted over a chicken-wire ground plane located to the south of the field-meter box. The preamplifier for this antenna was located immediately below the ground plane.

A block diagram of the Camera Pad 5 instrumentation for the launch of Apollo 13 is shown in Figure 8. At the top of the figure is the instrumentation for measuring ambient electric field. In planning the field-meter system, it was felt that wide dynamic range was required because of the variety of possible field variations postulated. To detect shorting of the ambient field by the rocket and plume, the system must be capable of producing substantial output in response to the fair-weather earth's field of 100 to 300 V/m. On the other hand, the system

FIGURE 7 DETAILS OF APOLLO 14 CAMERA PAD 5 INSTALLATION

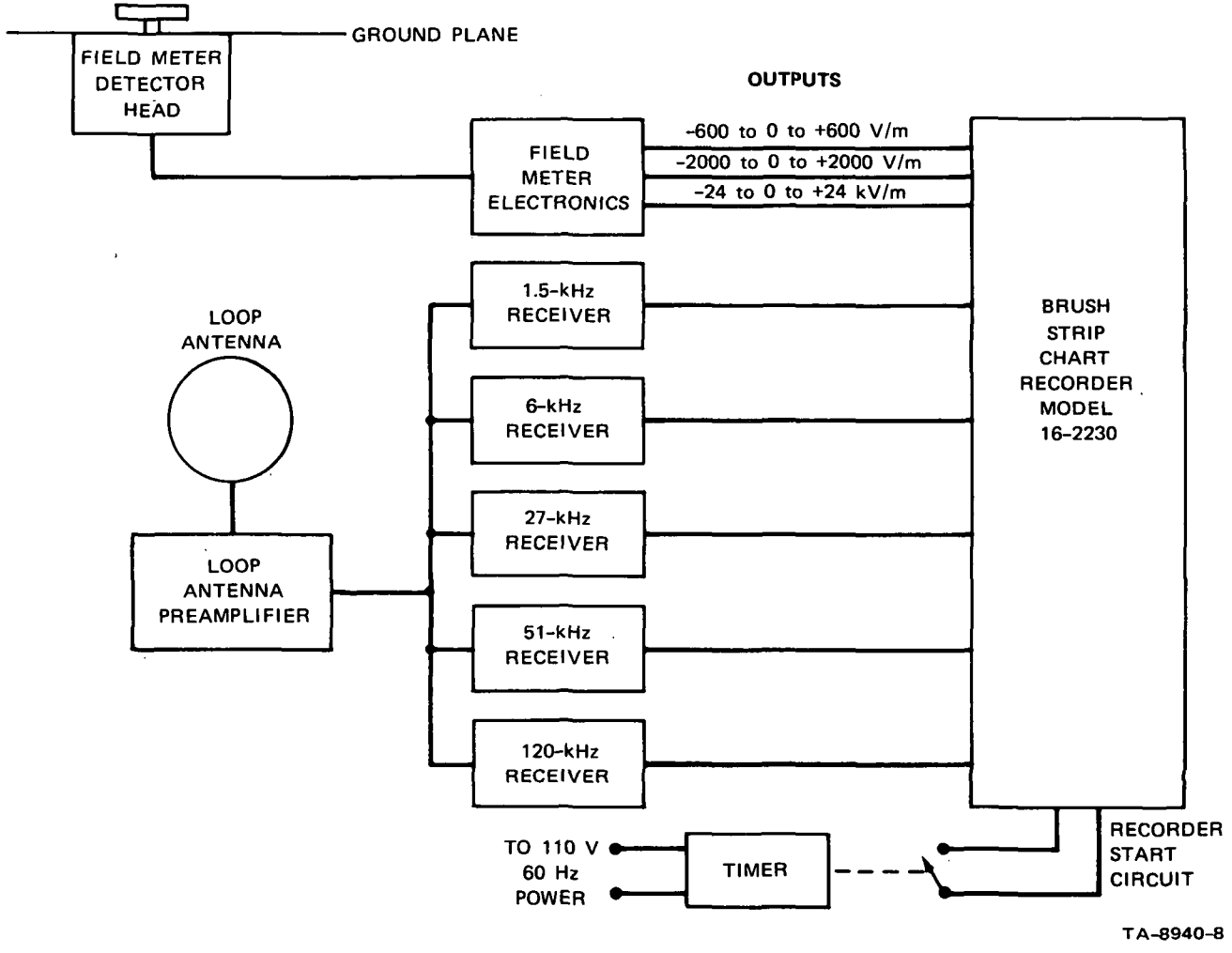

FIGURE 8 BLOCK DIAGRAM OF CAMERA PAD 5 INSTRUMENTATION FOR APOLLO 13

should not saturate in response to high charges on the rocket or exhaust products. Dynamic range was achieved by using three separate linear output channels with full-scale responses ranging from ±600 to ±24,000 V/m.

Lower in Figure 8 is the instrumentation for measuring LF noise. This consisted of a loop antenna and a broadband preamplifier that drove five fixed-tuned receiver channels. The output from each receiver (a dc voltage proportional to the input signal level) was fed to one channel of the strip-chart recorder. Dynamic range was achieved in this system by using a roughly logarithmic response in the receiver.

The clock timer at the bottom of the figure turned the recorder on roughly one hour before launch. The turn-on time and the strip-chart paper speed were adjusted to provide a period of baseline data prior to scheduled launch, and to assure adequate paper should the launch be "held" to the end of the launch "window." It should be noted that the only way in which an event could be timed with this system was by noting when the timer was set to turn on, and by measuring the paper consumed from turn-on to the event of interest. This is obviously not a precise procedure.

The more elaborate instrumentation system used at Camera Pad 5 for the launch of Apollo 14 is shown in Figure 9. The same field-meter system was used, but the gains were reduced somewhat based on the experience gained during the Apollo 13 launch. Also, provision was made for duplexing pulsed 500-Hz signals on the low-sensitivity field channel to provide range timing information on the strip-chart record. The LF noise receivers were unchanged from the Apollo 13 launch.

An important change in the Camera Pad 5 instrumentation system was the addition of the wideband tape recorder. This addition permitted the recording of wideband signals directly from the output of the loop-antenna preamplifier. These wideband data can be displayed later on an

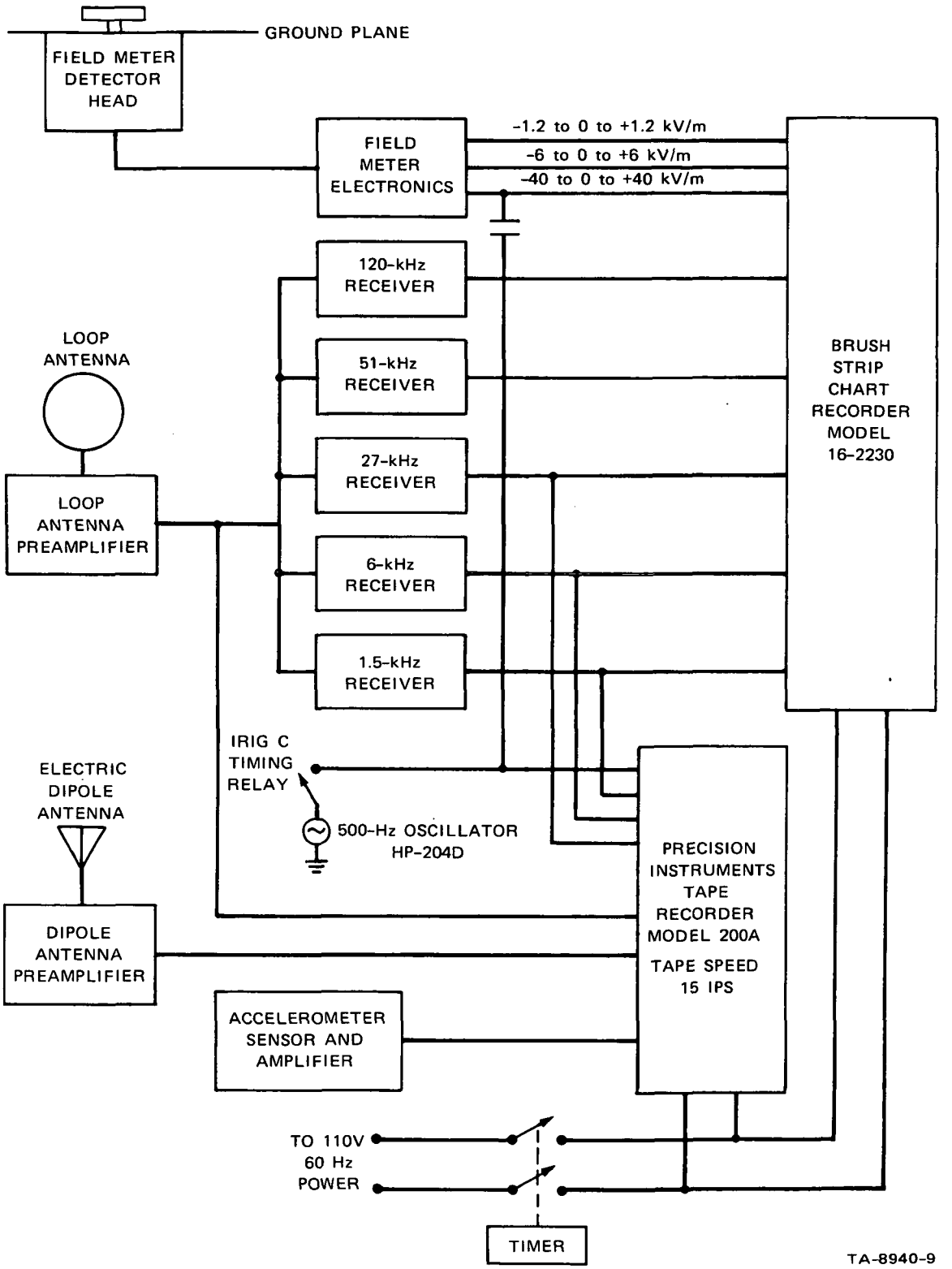

FIGURE 9 BLOCK DIAGRAM OF CAMERA PAD 5 INSTRUMENTATION FOR APOLLO 14

oscilloscope or otherwise processed to investigate the character of the LF radio noise observed during launch. (The recorded signals could even be fed to the receiver system as a check on the validity of the tape-recorded data.)

Also recorded on the tape recorder were the IF outputs from the three lowest-frequency receivers. It was felt that these data could prove useful in diagnosing the character of the noise sources.

With a wideband recorder available, it was felt that it would be useful to expand the noise sensors to include an electric dipole. Comparison of the noise records obtained with the two sensors would serve to validate the noise-measuring system, while systematic differences might provide additional insight into the character of the noise sources. The noise signal from the dipole was fed directly to one of the channels of the tape recorder.

Following the Apollo 13 launch there was some question regarding whether the receiver noise data might have been influenced by microphonics generated in the antenna preamplifier or the receivers by the acoustic noise associated with the launch. Accordingly, an accelerometer was included for the Apollo 14 launch to provide a time history of the vibration of the loop-antenna preamplifier case. This measurement would permit the comparison of receiver-noise onset and level with the mechanical vibrational levels existing at the time of interest.

Range timing information was supplied to the tape recorder by using a relay (operated from the range timing system) to key a 500-Hz oscillator signal that was recorded on one of the channels. Again, a timer clock was used to turn the system on prior to the scheduled launch time. For this launch it was necessary to turn the system on closer to the scheduled launch time, since the tape recorder could run for a total of only one

hour at the 15-ips speed required to give the required frequency response to record the desired broadband noise information.

In connection with the study of the electrification of Titan III-C rockets during launch, SRI developed and qualified a field-meter system capable of operating in an acoustic-sound-pressure environment of 160 dB (ref: 0.0002 dynes/cm^2) and 1360-peak-G shock-spectrum amplitude.[11] In planning for the Apollo 14 measurements, it was observed that these environmental specifications were comparable to the LUT-face environment during Apollo liftoff, and that this field meter should therefore be capable of surviving and providing useful data regarding vehicle potential during liftoff and the first few seconds of ascent. Provisions were made to install the field meter on the face of the LUT at the 340-ft level as shown in Figure 10. Various practical considerations entered into the decision to locate the field meter at this position. It was essential that the sensor be placed as high as possible on the LUT to maximize the data obtained prior to the passage of the engine nozzles. The 340-ft level was nearly at the top of the tower, and was the highest level at which available cabling existed suitable for carrying field-meter output signals to the NASA tape-recording system in the base of the LUT. A further reason for choosing the 340-ft level was that the LUT-face water-deluge system stops at a lower level and therefore there would be no possibility of the field meter being sprayed with deluge water during launch.

Additional details of the installation are shown in Figure 11. A sealed, nitrogen-purged box provided by NASA was modified to accept the field-meter electronics plug-in cards. The detector head was mounted in the lid of the box as shown in the figure. The entire assembly was fastened to the guard-rail structure of the LUT with the detector head facing outward. The piping and structural members on the face of the LUT surrounding the field meter serve to define a ground

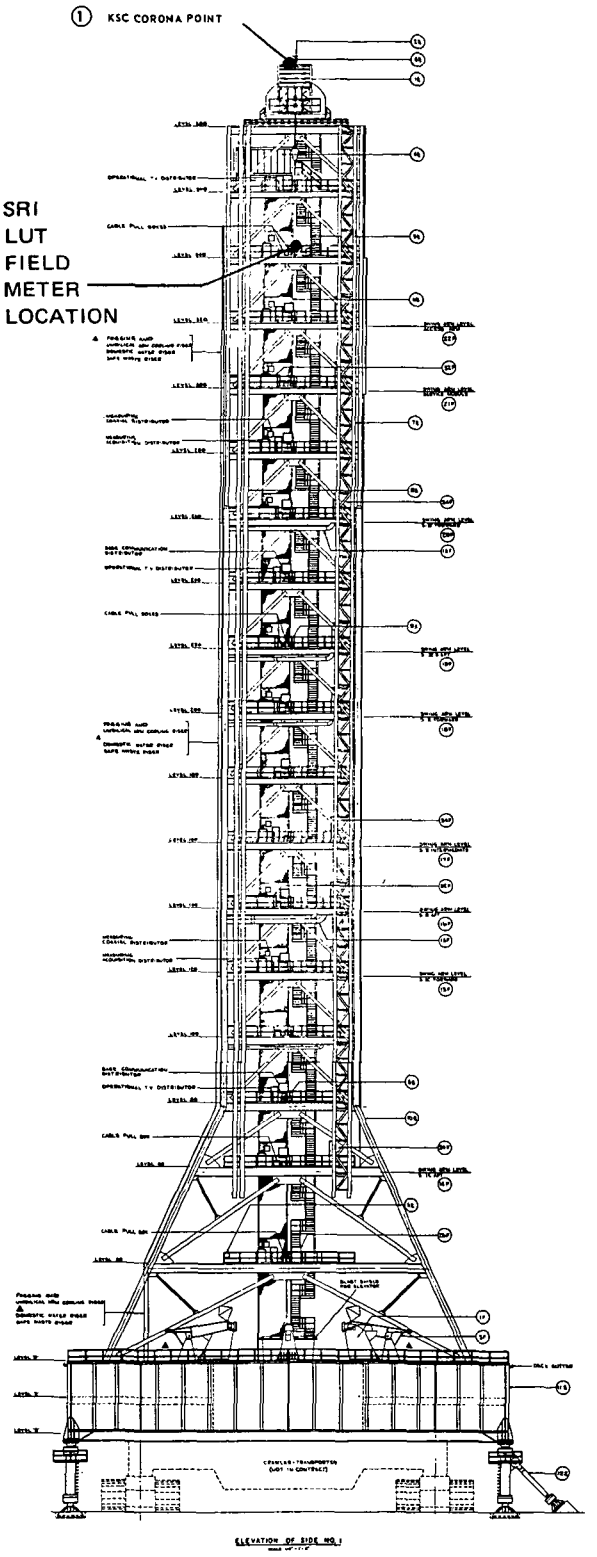

FIGURE 10 LOCATION OF FIELD METER ON LAUNCH UNBILICAL TOWER FOR APOLLO 14 LAUNCH

FIGURE 11 PHOTOGRAPH AT LUT FIELD-METER INSTALLATION FOR APOLLO 14 LAUNCH

plane, which simplifies the problem of interpreting the field-meter readings in terms of vehicle potential and ambient electric field. The field meter installed on the LUT was of the rotating-vane design. Movement of the grounded rotor shown in Figure 12 causes the stator to be alternately exposed to and shielded from the exterior environment. The alternating component of the stator short-circuit current in response to a true field is

$$I_f = \frac{1}{2} j\omega\epsilon_o EA \qquad (1)$$

where ω is the radian frequency with which the stator is covered and uncovered, ϵ_o is the permittivity of free space, E is the field strength of the electric field terminating on the stator (when the stator is uncovered), A is the surface area of the stator, and j is the imaginary unit $\sqrt{-1}$. The alternating component of the stator short-circuit in response to a convection current is nominally

$$I_c = \frac{1}{2} JA \qquad (2)$$

where J is the current density flowing toward the stator (when the stator is uncovered). Since the response to convection currents is 90 degrees out of phase with the response to an electric field, a coherent detector using a stable reference signal synchronized with the rate at which the rotor covers and uncovers the stator can be used to discriminate between the field response and the current response of the stator. (In the present field-meter system the reference signal is generated by an auxiliary set of vanes within the detector head.)

Similar field-meter systems using coherent detectors have often been used in airborne and ground field measurements because the coherent detector permits one to determine polarity of the field as well as field strength. In these systems, however, only the "in-phase" components of

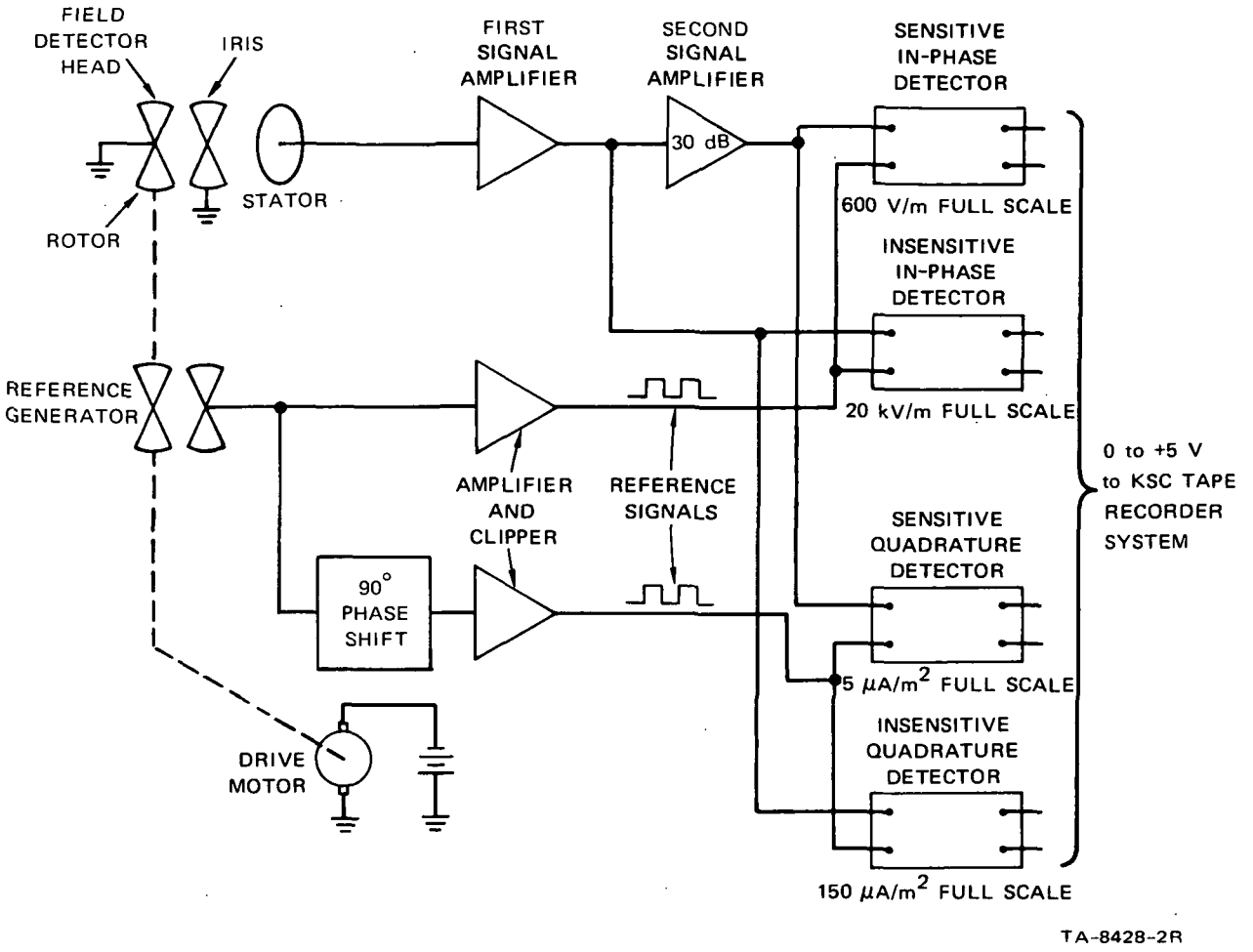

FIGURE 12 BLOCK DIAGRAM OF FIELD-METER SYSTEM

of the stator signal are normally detected. That is, the response to the electric field is detected, and the response to convection currents, which are usually small under fair weather conditions, is rejected. By using a second coherent detector adjusted to respond to stator signals in phase-quadrature with the field-produced signals, the response of the field meter to convection currents as well as electric fields can be obtained. Although this quadrature response of the field meter is not a very useful physical parameter, it does provide a basis for evaluating the behavior of the field meter in an ionized environment. In the present field-meter system, therefore, both the "in-phase" and "quadrature" components of the stator signal are detected.

As is indicated in the block diagram of Figure 12, the signal generated in the stator is amplified by two sets of amplifiers in series to provide two sensitivity levels for the system. The output from each signal amplifier is fed to two synchronous detectors, resulting in a high-gain and low-gain output for both E-field and J-field. As was indicated earlier, the reference signal is generated electrostatically by a vane structure mounted on the inboard end of the motor shaft. The E-field reference signal is fed directly from the reference stator to an amplifier-clipper that produces a square-wave output to the E-field synchronous detectors. To generate the J-field reference signals, the output from the reference stator is fed to a 90-degree-phase-shift circuit that drives the amplifier-clipper. The outputs from the field meter were adjusted to range from 0 to 5 V, to be compatible with the NASA data-recording system.

C. Calibrations

Each of the instruments used in the experiments was calibrated before and after the launch. The calibration was carried out after the instrument was installed for launch, and consisted of injecting a known signal at the sensor and operating the normal recording system to record the data. In this way, every element of the system from the sensor to the recorder was included in the calibration loop.

The field meters were calibrated by mounting a 1-ft-square aluminum sheet 10 cm above the sensor ground plane and applying a stepped voltage of known value between the ground plane and the calibrating plate. Noise-measuring system calibrations were accomplished by injecting known RF currents into the preamplifier input of the antenna in question.

In addition to the on-site calibrations of the instrumentation, it was necessary to carry out certain supplementary measurements in the

laboratory essentially to obtain analog solutions to electrostatic-field problems. For example, it was necessary to determine the field perturbation caused by the presence of the box on which the ground field-meter sensors were installed. This was done using the arrangement of Figure 13.

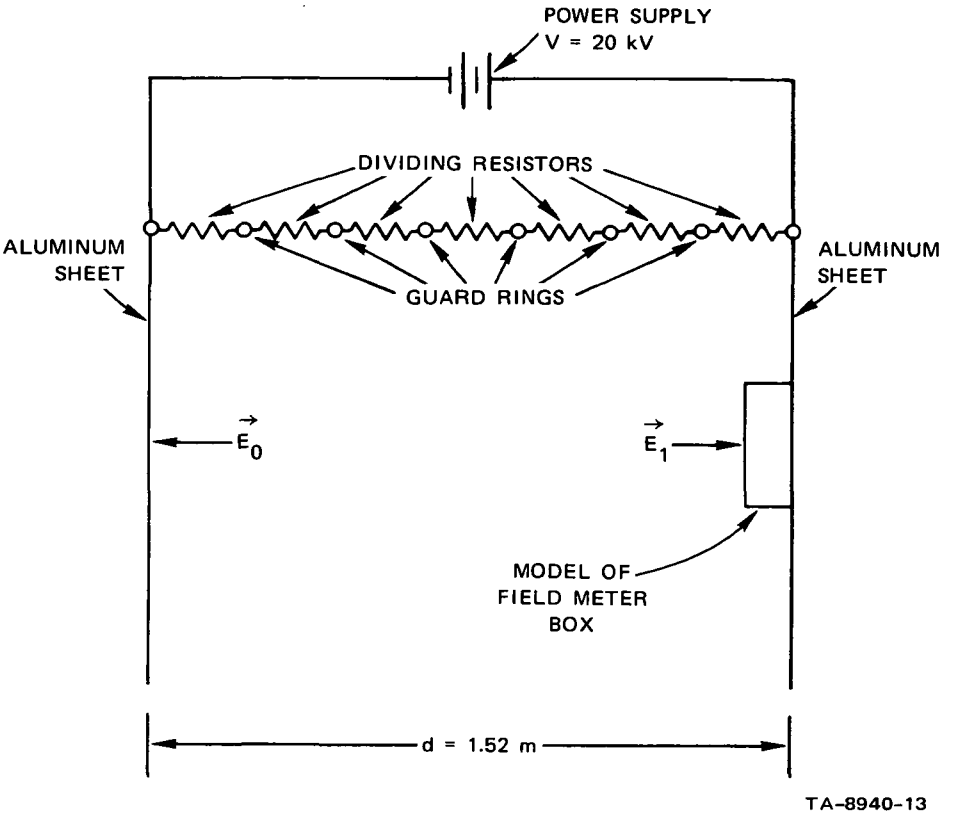

FIGURE 13 LABORATORY MEASUREMENT SCHEME TO OBTAIN RELATIONSHIP BETWEEN LOCAL FIELD AND AMBIENT FIELD

Here a uniform field E_o is established between a pair of parallel plates (guard rings and divider resistors are used to minimize field fringing). A model of the field-meter box is placed on one of the end plates. The field E_1 at the top of the box is measured by touching a small conducting probe to the point at which the field measurement is made. The probe picks up a charge proportional to the magnitude of the electric field at the contact point. This charge is transferred to an electrometer bucket and measured. By repeating the measurement in a region of known field such as E_o, one obtains a relationship between charge and field as $E_1/E_o = 1.6$.

The setup of Figure 13 was also used to determine the relationship between ambient field and LUT-face field at the field-meter location. A model of the LUT was attached to one plate of the electrostatic case and charge-transfer measurements were made. It was found that $E_o/E_{LUT} = 0.183$.

The relationship between vehicle potential V and electric field E at the LUT field-meter position was determined using the setup of Figure 14.

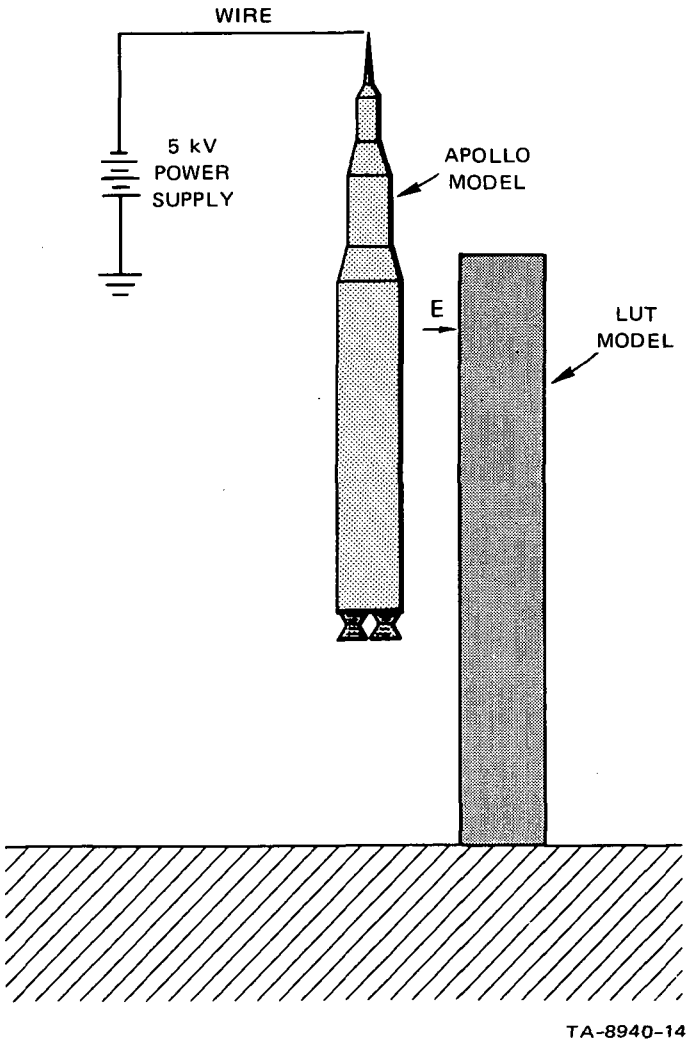

FIGURE 14 LABORATORY SETUP TO OBTAIN RELATIONSHIP BETWEEN VEHICLE POTENTIAL AND LUT FIELD-METER READING

Here a model of the LUT is placed on the floor of the laboratory, and provisions are made to charge a model of the Apollo, which can be positioned at various heights above ground along the trajectory followed during liftoff. Charge-transfer measurements of E at the scaled LUT field-meter location are made as the rocket model is moved past the LUT. The results of this measurement are shown in Figure 15. The coupling between the rocket and the field meter remains relatively constant while some part of the body of the rocket is opposite the field-meter position. Once the nozzles reach the field-meter height, the coupling decreases abruptly. (It should be noted that the Apollo vehicle is scaled as an isolated conducting body, with this modeling scheme.)

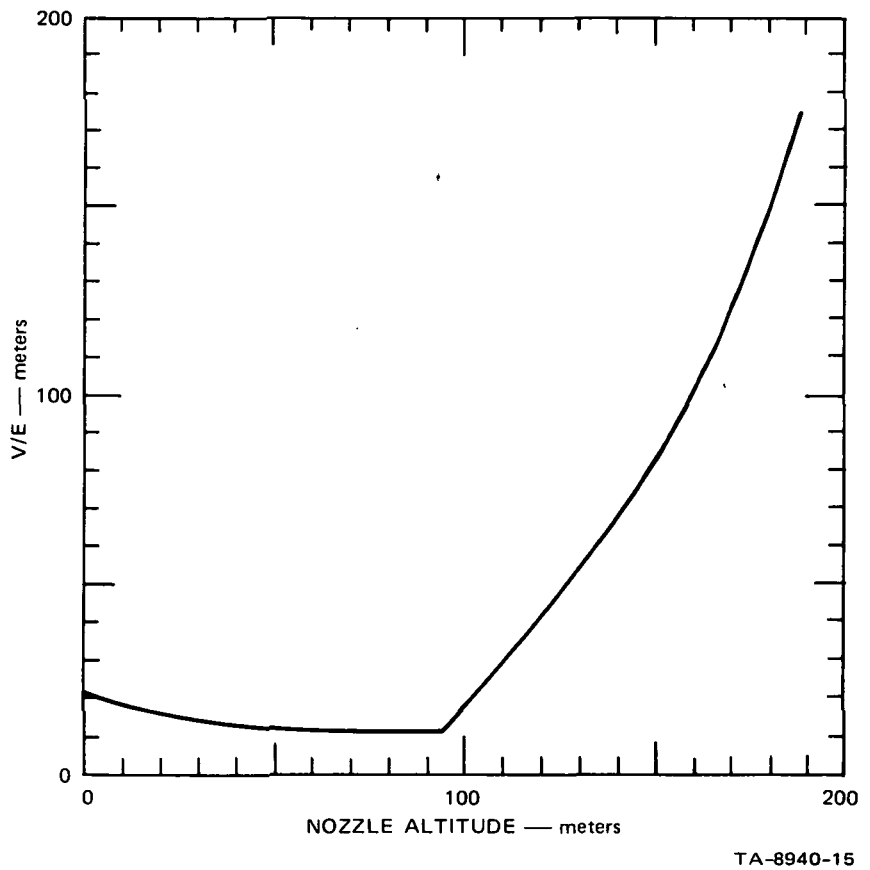

FIGURE 15 RELATIONSHIP BETWEEN ROCKET POTENTIAL AND LUT-FACE FIELD AT FIELD-METER POSITION

III RESULTS OF EXPERIMENTS

A. Electric-Field Measurements

1. Apollo 13

Excellent records of vertical-electric-field variations were obtained at Camera Pad 5 as shown in Figure 16. The field perturbation following launch was initially positive and rose to a maximum of almost 1200 V/m about 25 s after the initial perturbation; the direction of field change reversed until a negative peak of some 300 V/m was reached at a time of approximately 115 seconds; thereafter the field gradually returned to the unperturbed value. This same general behavior of the electric field was observed by NMIMT[10] at their Camera Pad 1 location, as shown in Figure 17, where their data are plotted for comparison with the SRI Camera Pad 5 record. This agreement in the records is not surprising since, as shown in Figure 3, the two installations were quite symmetrically located both with respect to the flame trenches and with respect to the ground wind shown in the figure.

The SRI Camera Pad 4 record shown in Figure 16 also consisted of a generally positive excursion followed by a negative excursion. At this station, however, there were large superimposed fluctuations. (The exact details of these fluctuations are not entirely consistent among the several sensitivity ranges. This stems from the fact that the Rustrak recorders used at this station have a complicated response to transients whose characteristic period is small compared to the meter response time.) After the launch, a quantity of gravel and dust debris was found on the surface of the aluminum ground plane around the field

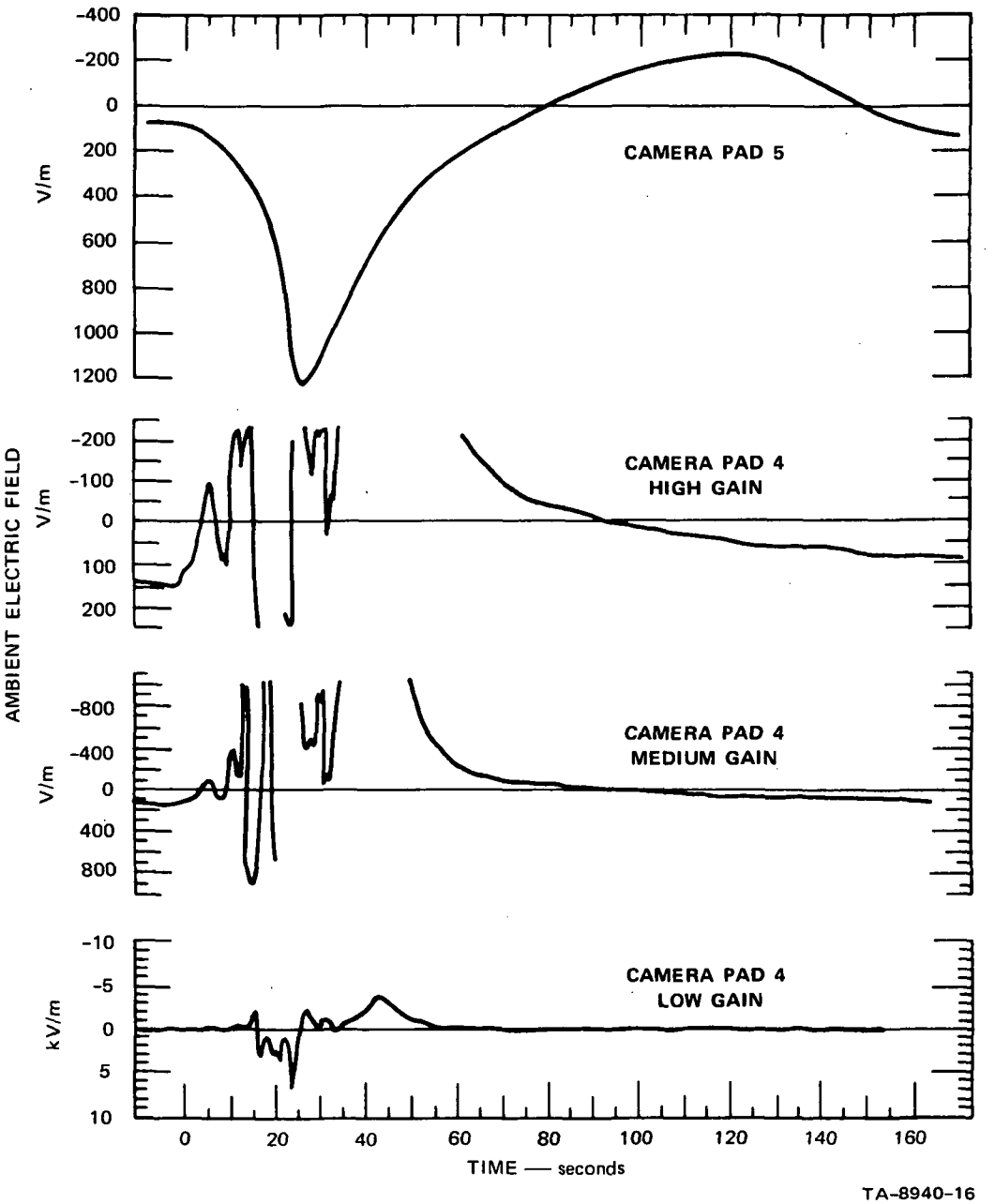

FIGURE 16 FIELD-METER RECORDS FROM APOLLO 13 LAUNCH

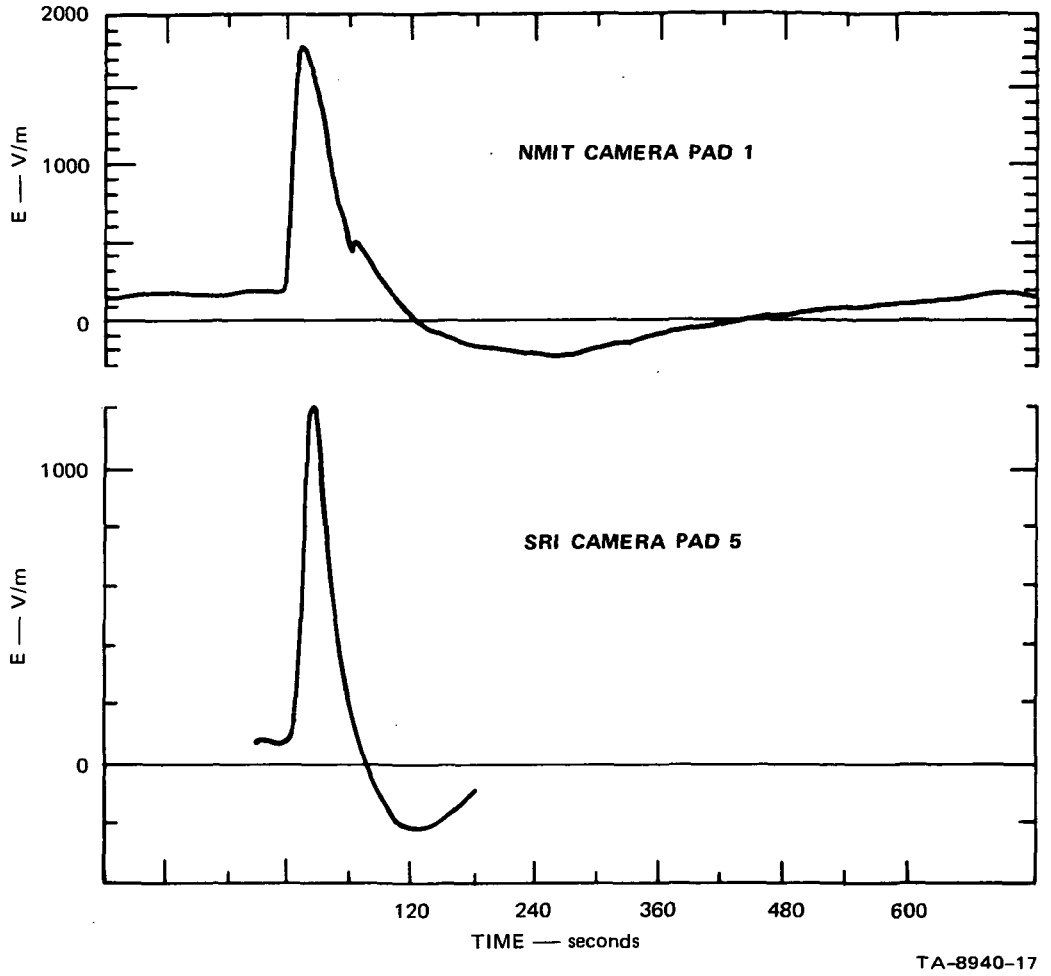

FIGURE 17 COMPARISON OF SRI AND NMIMT FIELD-METER DATA FROM APOLLO 13

mill. No such debris was found at Camera Pad 5. Consequently it is plausible to associate the occurrence of the field fluctuations with the presence of this debris.

At the slidewire and crawlerway sites, the recorders, which had to be started well prior to launch time because of time restrictions on access before launch, had unfortunately stopped before liftoff. However, it was noted that on the stationary parts of the records there were substantial positive and negative field perturbations greater than anything found on the moving portion of the records. Comparison with

the records from Camera Pads 4 and 5 confirmed that the only large field perturbations were those accompanying launch. Consequently, the peak excursions on the records at the slidewire and crawlerway sites could be confidently associated with the maximum field perturbations occurring at launch.

The Camera Pad 5 field-mill record is not consistent with the simple electrostatic model involving an uncharged rocket and no charged exhaust clouds illustrated in Figures 1(b) and 1(c). With this model, the magnitude of the measured field should increase after launch, but its polarity should not change.

Similarly, the field-meter record is not consistent with the model of Figure 1(d) in which a highly conducting plume thousands of feet long reduces the magnitude of the field to distances of thousands of feet from the launch point. The data of Figure 17 show a clear increase in the magnitude of the electric field at the time of launch. Although in the two higher-gain Camera Pad 4 records of Figure 16 the magnitude of the electric field decreased for the first few seconds after launch, this decrease is associated with an ultimate reversal in polarity and therefore does not constitute a field change of the type predicted by the model of Figure 1(d).

An investigation was next made of the degree to which the measured static-electric-field data fit the model of Figure 2 in which the rocket is assumed to be highly charged by the action of the engines. (The form of the field variation observed on the launch of Apollo 13 is apparently consistent with this model if we assume that the vehicle charged positively at liftoff, thus generating the positive field excursion as the rocket climbed. The subsequent negative excursion can be associated with the negatively charged exhaust products left

behind by the rocket.) The field E produced on a ground plane by a charged body located a distance h above the ground plane is given by

$$E = \frac{2Q}{4\pi\varepsilon_o} \frac{h}{(h^2 + r^2)^{3/2}} \tag{3}$$

where

Q = Charge on body

$\varepsilon_o = 8.85 \times 10^{-12}$ farad/meter

r = Distance from launch point to measurement point.

The field E is maximum when $\partial E/\partial h = 0$. Carrying out the differentiation gives E_{max} when $h = r/\sqrt{2}$. For this value of h, the maximum value of field is

$$E_{max} = \frac{Q}{\pi\varepsilon_o r^2} \frac{1}{3\sqrt{3}} \quad . \tag{4}$$

For the Camera Pad 5 field meter that is 400 m from the launch pad, maximum field should occur* when h = 282 m. From Figure 18, we find that the rocket reaches this altitude in about 16 s after liftoff. Most unfortunately, no indication of liftoff time could be included in the experimentation for Apollo 13. Accordingly there is a substantial uncertainty in relating the times of various features on the records to liftoff. The NMIMT record[10] from Camera Pad 1 (Figure 17) shows a quite sudden increase in field that only lasts about 18 s from onset to maximum; since this record was taken 415 m from the launch site,

* Assuming that the charge on the vehicle is constant. This assumption cannot be checked without instrumentation on the vehicle, and may be quite unrealistic.

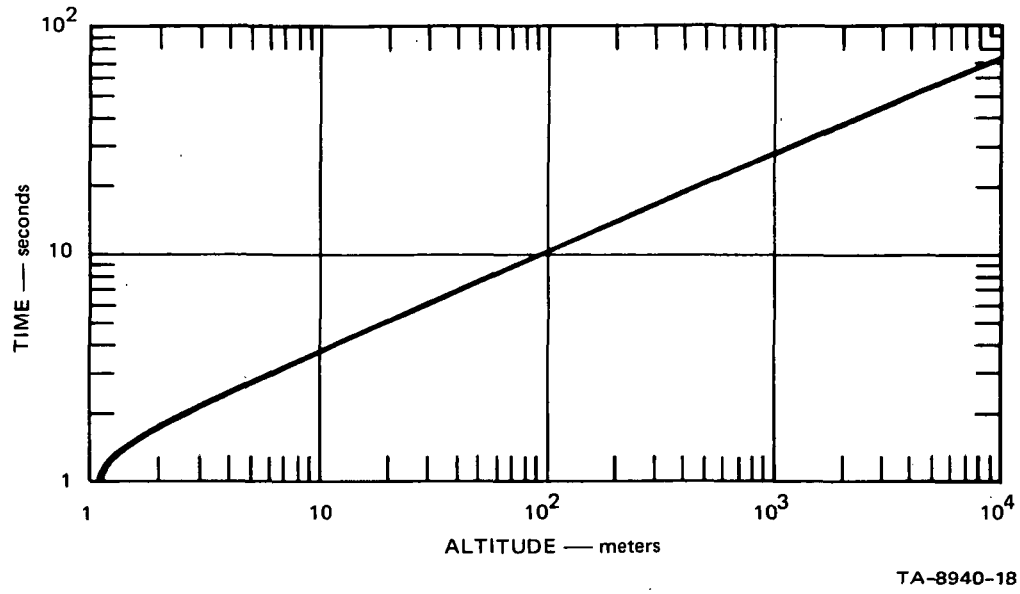

FIGURE 18 ALTITUDE-vs.-TIME HISTORY OF APOLLO 13 ROCKET

the field maximum using Eqs. (3) and (4) and Figure 18 should occur 17 s after liftoff. Thus it is a quite plausible interpretation of the NMIMT record to assume that the onset of the positive field change is associated with liftoff, and that the form of the perturbation, at least to maximum, is dominantly controlled by charge on the vehicle as it ascends. The SRI record from Camera Pad 5 (Figure 16) is rather more complicated; following onset, (1) the rate of field increase is quite small for almost 20 s, but (2) there is then a fairly abrupt change in slope, and (3) maximum is attained some 15 s later. It is tempting to identify Item 1 with processes occurring prior to liftoff, Item 2 with liftoff, and Item 3 with the influence of positive charge carried on the ascending vehicle. The time of 15 s from liftoff to maximum would then correspond excellently with the 16 s predicted by the analysis based on Eqs. (3) and (4) and Figure 18.

Suppose we assume that the maximum field change ΔE = 1200 V/m at Camera Pad 5 occurs 16 s after liftoff when the rocket is at h = 282 m; substitution into Eq. (4) then yields $Q = 2.76 \times 10^{-2}$ coulomb. Similar calculations were carried out for the line of field meters extending to the west of the pad and for two of the NMIMT sites. The results of these calculations are given in Table 1.

The various values in the last column of Table 1 are in quite good agreement. The time histories of the records from Camera Pad 5 and Camera Pad 1 are not incompatible with the hypothesis that the field-change to maximum is due to positive charge carried on the vehicle. For NMIMT Site 3 there is a discrepancy of at least 20 s; this could possibly be explained by postulating a charge variation on the vehicle, by envisaging other sources of charge, and so on.

The data from Camera Pads 1 and 5 that give $Q \sim 3 \times 10^{-2}$ coulomb appear to be the most reliable. It is interesting to calculate the vehicle potential that this value of charge implies. The free-space capacitance of a prolate spheroid[12] is

$$C = \frac{8\pi\epsilon ae}{\ln \frac{1 + e}{1 - e}} \tag{5}$$

where

a = Semi-major axis of the spheroid

e = Eccentricity = $\sqrt{1 - \left(\frac{b}{a}\right)^2}$

b = Semi-minor axis of spheroid.

Table 1

ESTIMATE OF CHARGE Q CARRIED BY APOLLO 13 AFTER LAUNCH

Site	Maximum Positive Field Perturbation ΔE(V/m)	Distance From Launch Point (m)	Time of Maximum After Liftoff (s)		Estimate of Q (coulomb)
			Expected [Theory of Eqs. (3), & (4), & Fig. 18]	Indicated on Record	
Camera Pad 5	1200	400	16	15-35	2.8×10^{-2}
Slidewire	700	790	22	--	6.4×10^{-2}
Crawlerway	100	1750	31	--	4.5×10^{-2}
Camera Pad 1 (NMIMT)	1550	415	17	18	3.8×10^{-2}
Site 3 (NMIMT)	250	1500	29	50-65	8.1×10^{-2}

It is convenient to approximate the Apollo 13 vehicle by a prolate spheroid with a = 50 m and b = 5 m, and to evaluate Eq. (5) for the resulting free-space capacitance. Such a calculation yields Capacitance = 1.84×10^{-9} farad, which implies that with a charge of 3×10^{-2} coulombs the vehicle potential is 1.6×10^{7} V. This value of potential seems large, but it should be observed that the equilibrium potential for an aircraft or rocket is determined when the engine-charging current is balanced by the corona current from the aircraft. With a conventional commercial jet aircraft[6] this equilibrium potential can approach 10^{6} V. For the large engines of the Saturn rocket one would expect the engine-charging current to be far larger than with jet aircraft; furthermore, since there are probably more effective "roughnesses" on an aircraft than on the rocket, the corona current for a given voltage will be proportionately greater for the former than for the latter case. Both these effects will tend to make the equilibrium potential for the Saturn rocket substantially larger than in the case of the jet aircraft; several million volts does not therefore seem an impossible estimate for the Saturn equilibrium potential.

Brook et al.[13] have estimated the maximum charge (and consequently potential) that can be acquired by a prolate spheroid simulating the Apollo vehicle. Their analysis assumes that as soon as the breakdown-field value* is exceeded at the end of the spheroid (the location of highest field development) there can be no further increase in the charge (and potential) on the vehicle. This assumption seems physically incorrect and quite at variance with experimental results. Breakdown will first occur as corona initiated at the corona onset potential. However, the onset potential is not the maximum potential that can

---

* As determined for breakdown between plane parallel electrodes.

develop on an object in corona. Indeed, it is well established that stable corona discharges are maintained from such diverse objects as aircraft, laboratory discharge needles, and points at the earth's surface during thunderstorms, for potentials approaching a hundred times the corona onset value. Furthermore, when corona is occurring from a pointed object the field at the point is considerably greater than the parallel-plate breakdown value; also, the region of substantially enhanced field, although influenced by space charge, usually extends to some distance from the surface of the point.

The charge, Q, and the field at the tip, E_T, of a prolate spheroid are related by[14]

$$Q = 4\pi\epsilon_o b^2 E_T \quad .$$

If, following Brook et al.,[13] we assume that E_T cannot exceed the parallel-plate breakdown value (3×10^6 V/m at sea level; 2.4×10^6 V/m at 6000 feet) then for b = 5 m we deduce a maximum sea-level value for Q of 8×10^{-3} coulomb; since Capacitance = 1.84×10^{-9} farad, the corresponding potential is approximately 4×10^6 V. Reasons have been given in the proceding paragraph for questioning the above assumption, and indicating that in reality the vehicle can carry much higher charges and potentials than those deduced by Brook et al.[13] Certainly it seems entirely possible for a potential of 2×10^7 V to reside on the vehicle with no worse consequences than copious corona from roughnesses on the surface. There would be incipient streamers from these roughnesses, but in the absence of a general ambient field[3] approaching 10 kV/m the streamers would not develop.

With a potential of several million volts the Saturn vehicle, as already indicated, may be expected to be in corona, the corona onset being very soon after liftoff. The corona should generate radio noise.

The Apollo 13 radio-noise records (discussed later) strongly supported this picture.

The final model that might be invoked to explain the observed field variations is that of Figure 1(e), in which the exhaust products, clouds, and dust stirred up by the launch are all charged to some degree and polarity, and these charges are dominantly responsible for the electrostatic fields observed at launch.

The above discussion illustrates the state of understanding of the electrostatic processes associated with an Apollo launch shortly after the launch of Apollo 13. When Apollo 14 ground experiments were being planned it was possible to conclude that the rocket did not have the electrical appearance of a giant conductor producing large-scale shorting of the ambient field extending to thousands of feet. It was also clearly evident that high electrostatic charges were generated by the launch. If one argued that all of the positive charge was stored on the launch vehicle, with the corresponding negative charge being gradually dispersed in the exhaust clouds, high vehicle potentials resulted, but the explanation for the form of most of the field variations was gratifyingly simple and straightforward. If, on the other hand, one argued that all the charge resided on the exhaust products and clouds, it would be necessary to devise explanations for the fact that both positive and negative charges were observed, and for the unusually large negative charges at certain locations (e.g., the dust-influenced Camera Pad 4). It was noted during the launch of Apollo 13 that certain of the exhaust-generated clouds developed very rapidly and had reached heights comparable with that of the LUT by liftoff. Thus, if these clouds were indeed charged, their effects should be apparent before any perturbations due to charge on the vehicle.

Review of the above information indicated that defining vehicle potential at and soon after launch should receive high priority in the Apollo 14 experiments. It was also observed that the exhaust products from the flame trench, especially to the south, appeared to have interesting properties and should be investigated more closely. Finally, it was argued that accurate timing information was essential if the electrical effects were to be correlated with launch events or with themselves. Accordingly, the instrumentation system was expanded for the launch of Apollo 14, as discussed in detail in Section II-B. Specifically, the LUT field-mill was added, an additional station was set up to the south, and timing signals were included.

2. Apollo 14

Field-meter data from the SRI Apollo 14 experiment are summarized in Figure 19. (For the Apollo 14 measurements, timing signals were provided to all recorders so that there is no question regarding proper time relationships between the various sets of data.) Good records were obtained at all sites except Camera Pad 4; here the recorder failed. In general, the field magnitudes are lower than those obtained at corresponding locations during the Apollo 13 experiment. For comparison, the field-meter records obtained at Camera Pad 5 on the two launches are plotted together in Figure 20. It is evident that the peak field obtained at this location on Apollo 14 is roughly 1/5 that obtained on the Apollo 13 launch. A further difference between the two launches is that on Apollo 13 the initial positive deflection was followed by a negative overshoot, whereas on Apollo 14 the field decayed monotonically following the initial positive deflection.

In general, the SRI data show a positive field change at the time of launch at all stations. The NMIMT records for Apollo 14 show widely varying fields of much higher magnitude than those obtained by SRI

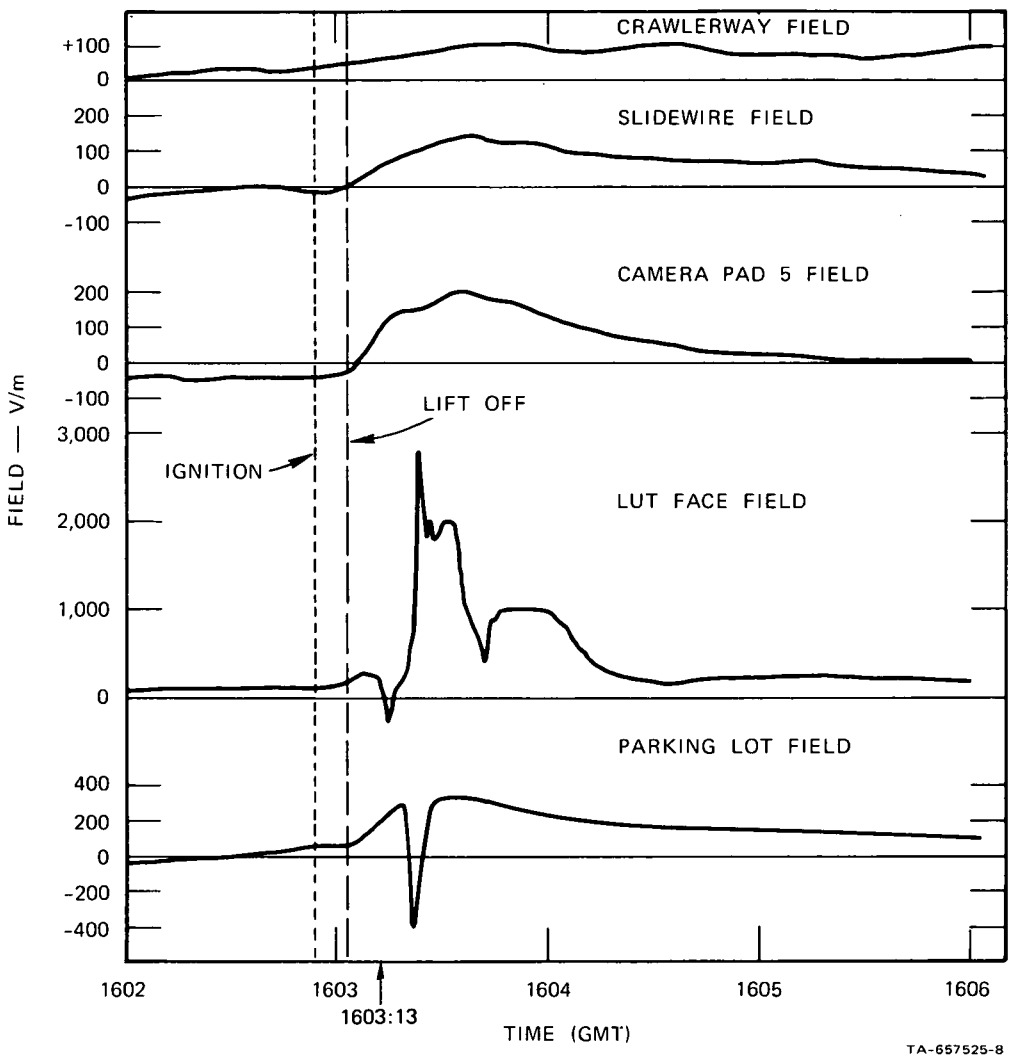

FIGURE 19 SRI FIELD-METER DATA FROM APOLLO 14

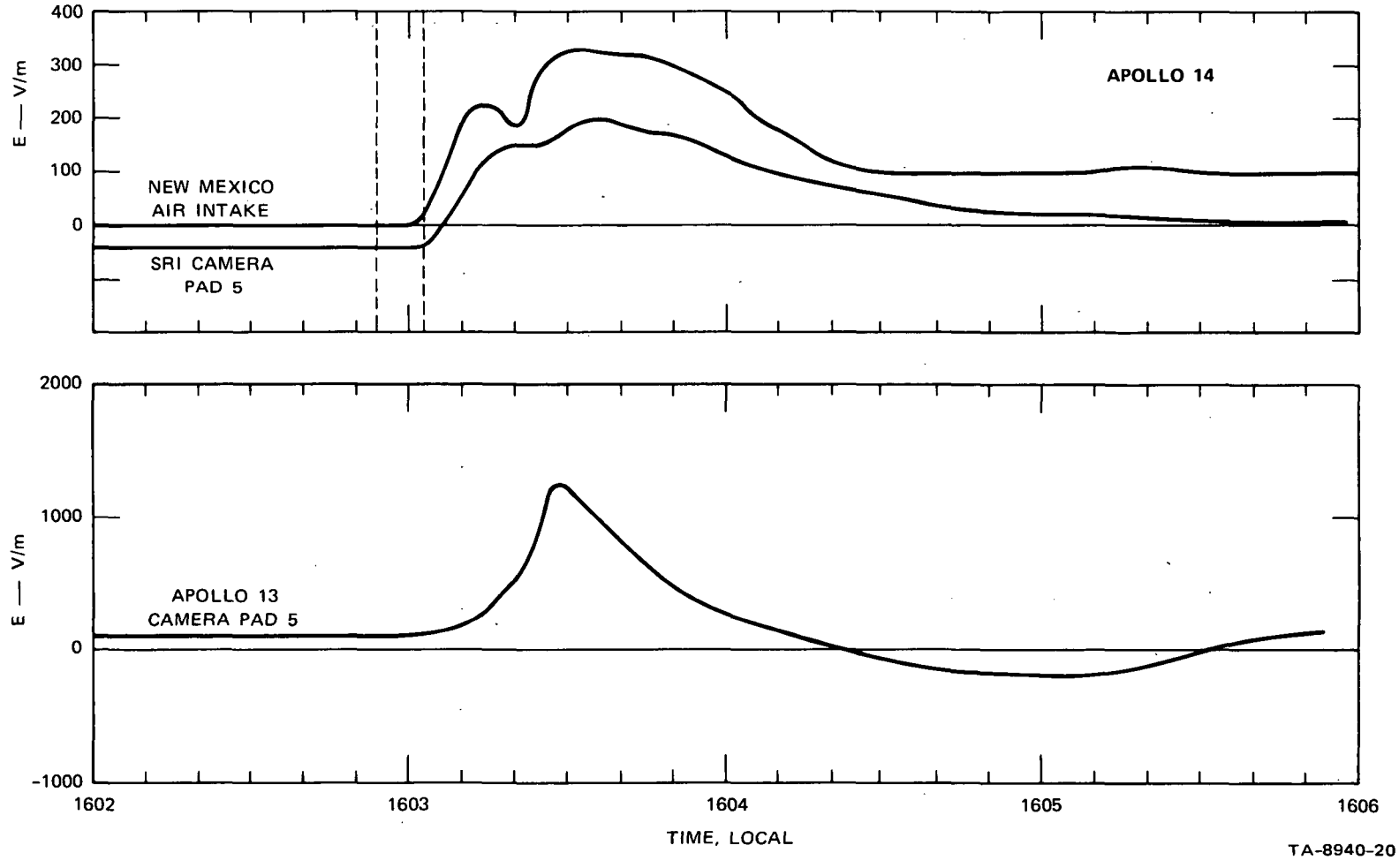

FIGURE 20 COMPARISON OF FIELD-METER DATA

(more like the records obtained by SRI on Apollo 13). At the one nearly common location, however (NMIMT air intake and SRI Camera Pad 5), the records are in reasonable agreement as is shown in Figure 20. Thus it appears that the great disparity in the types of records obtained stems from real physical effects, and not from instrumentation difficulties.

Upon first inspecting the SRI Apollo 14 data, one is struck by the fact that all the field changes at launch, including the LUT measurement, are positive. As in the case of Apollo 13, this form of field variation can be simply explained by arguing that the vehicle becomes positively charged as it leaves the pad, and that this positive charge on the vehicle is responsible for generating the positive changes in the field observed on the ground around the launch pad. Again, it is instructive to carry out calculations to test this simple model. At Camera Pad 5, ΔE_{max} = 250 V/m at 35 s after liftoff, at which time the vehicle is at a height of 1344 meters. Substituting these values into Eq. (3), we find that the charge on the vehicle must be $Q = 2.9 \times 10^{-2}$ coulomb. For a vehicle capacitance of 1.84×10^{-9} farad, the above charge implies that the vehicle potential would have to be $V = 1.6 \times 10^{7}$ V. From the LUT field-meter record of Figure 19 at time T = 1603:13, when the rocket nozzles reached the LUT field meter (at the 340-foot level), the highest field intensity measured was 300 V/m. Even extrapolating the initial rate of rise to T = 1603:13 we find that the field would be 600 V/m. Using the results of the model measurements illustrated in Figure 15 we find that, with the vehicle at the 340-ft level, the LUT face field and vehicle potential are related by V/E = 11 meters. Thus, the rocket potential is less than 600 × 10 = 6000 V. Returning to Figure 19, we find that at T = 1603:13, the Camera Pad 5 field has reached roughly half its final peak value, which means that, if we were to account for the field changes entirely on the basis of charge on the rocket, the rocket potential at this time would have to be of

the order of megavolts. The low LUT field-meter reading thus argues that high vehicle charge in the initial ascent stages is not the mechanism by which the observed field changes were generated.

It is appropriate at this time to give some consideration to the degree of confidence one can place in the LUT field-meter data. The field meter installed on the LUT was a special heavy-duty unit qualified to a 160-dB acoustic environment and to a 1360-G peak shock.[11] In the qualification test program the unit functioned within calibration limits during the application of the environment. The particular unit installed on the LUT was functioning within calibration limits upon being returned to SRI following the Apollo 14 launch. The LUT field-meter data show no sign of breakup except for the period between 1603:18 and 1603:22--by this time the rocket was well above the top of the LUT. Immediately prior to the launch, the LUT face field was +100 V/m. From the model measurements of Figure 13 this means that the ambient field in the vicinity of the LUT was $0.183 \times (100) = +18.3$ V/m. This value is compatible with the general field values measured prior to launch of Apollo 14. (These were of the order of 100 V/m or less and varied with time and from site to site; this variation is to be expected under the rather disturbed weather conditions prevailing at launch time.) Thus there is no obvious reason to distrust the data from this instrument. It must be concluded, therefore, that while it was passing the LUT, the Apollo 14 potential was 6,000 V or less.

We are left with the necessity for explaining the observed phenomena, assuming that the rocket potential is of the order of 10 kV or less at least until it clears the LUT. About the only mechanism left to explain the field changes is charges residing on the exhaust clouds. Inspection of the available movies of the launch indicates that these clouds have built up to considerable heights (above the LUT) during the nine seconds of engine operation before liftoff. Inspection of the field-meter records

in Figure 19 shows, however, that there was no substantial change in field at any of the sites prior to liftoff; the NMIMT records show a similar pattern. This argues that the exhaust clouds were uncharged while the rocket was on the ground but became progressively more and more charged during the initial stages of vehicle ascent. There are reasons for believing that exhaust-cloud charging occurring as the result of particle and droplet impingement on the flame deflector and flame trench could show this behavior. When the rocket is on the ground, the energy in the exhaust is sufficient to vaporize all of the water spray so that, during the time that it is in the flame trench, the trench exhaust is in the vapor state and produces no charging upon impact with the trench. As the rocket lifts off, the temperature of the exhaust in the trench decreases so that some of the water spray remains in liquid form and becomes charged upon impact with the trench. Similarly, the character of solid particles contained in the rocket exhaust itself changes with distance from the nozzles. Near the nozzles, carbon exists as small incandescent particles. As one moves away from the nozzles, the carbon particle size increases, and the particles are no longer incandescent. Thus, charging of these particles on impact with the flame trench would also be expected to change with the distance of the rocket above the pad.

The clouds generated during launch have a complicated structure the details of which may vary from launch to launch. However, three main cloud complexes may be identified; their characteristics are summarized in Table 2.

The only records showing substantial (>1 kV/m) negative fields sustained for many seconds are those from Camera Pad 4 (SRI) for Apollo 13, and from Camera Pad 3 (NMIMT) for Apollo 14. In addition, short-lived but quite definite excursions of negative field were recorded for Apollo 13 at Camera Pad 4 (SRI), and for Apollo 14 at

Table 2

APPROXIMATE CLOUD CHARACTERISTICS DURING LAUNCH OF APOLLOS 13 AND 14

Cloud	Origin	Time (s)	Vertical Height of Cloud (m)	Horizontal Elevation of Cloud Extent (m)	Horizontal Orientation of Cloud	Vehicle Height (m)	Remarks
North	Interaction of exhaust with north flame trench and its water systems. Water on from 60 s before ignition.	5	30	200	Almost along trench	0	Cloud of homogeneous light gray appearance
		10	70	400		3	
		15	140	500	Transitional	40	
		20	200	600	Almost along wind direction	150	
		30	320	600		600	
		40	420	600		1,500	
		50	500	600		2,700	
		60	580	600		4,500	
South	Interaction of exhaust with south flame trench and its water systems. Water on from -60 s before ignition.	5	100	250	Almost along trench	0	Inhomogeneous appearing cloud. Upper part whitish gray, lower part darkish gray.
		10	160	500		3	
		15	250	600		40	
		20	330	700	Transitional	150	
		30	440	700	Almost along wind direction	600	
		40	550	700		1,500	
		50	640	700		2,700	
		60	740	700		4,500	
Central	Interaction of exhaust with LUT structures and their water systems. System 1 (5,500 gal/min) on from 10 s to 42 s after ignition; System 2 (24,000 gal/min) on from 42 s to >100 s after ignition; Deluge (6,000 gal/min) from 5 s to >100 s after ignition.	5	10	10	Around LUT	0	Cloud of homogeneous light gray appearance
		10	30	40		3	
		15	50	100	Transitional	40	
		20	70	100	Almost along wind direction	150	
		30	100	100		600	
		40	130	100		1,500	
		50	160	100		2,700	
		60	190	100		4,500	

Camera Pad 1 (NMIMT) and at the parking lot (SRI). It is noteworthy that both Camera Pads 3 and 4 are likely to be much influenced by the south cloud; also, the relative directions of the surface winds were such that for Apollo 13 the south cloud would pass close to or over Camera Pad 4, while for Apollo 14 the south cloud actually passed above Camera Pad 3.[15] Furthermore, the sites at Camera Pad 4 after Apollo 13 and Camera Pad 3 after Apollo 14 both experienced a deposition of particles following the launches. All these effects strongly suggest that the south cloud contains, at least in its lower portions, particulate matter carrying negative charge, and that the fallout of these particles could have accounted for the short negative field excursion at the parking lot. Brook and Moore[15] have suggested that there is little cooling water in the south flame trench during launch, and it is for this reason that the particulate matter is produced. There are some indications, such as the very disturbed early part of the record for Apollo 13 from Camera Pad 4, that the electrical structure of the south cloud cannot be simply represented by negative particle charge in the cloud base above. The different appearance of the top and base of the cloud indicates a possible bipolar structure with positive charge in the upper parts of the cloud. The record from the parking lot (SRI) strongly supports a bipolar structure for the south cloud. The general change of field is positive, reaching +300 V/m some 40 s after ignition. This change cannot plausibly be ascribed to the north cloud since Camera Pad 5 (SRI) and the Air Intake sites (both stations substantially closer to the north cloud at early times than the parking lot) show smaller positive field changes than that at the parking lot. At $t = 40$ s, the south cloud is about 500 m from the parking lot site and with a mean height of perhaps 500 m (Ref. 15). A positive charge of some 10 millicoulombs located at this position would account for the observed field-change at the parking lot.

The north-cloud motion is initially along the north flame trench until it reaches approximately to the perimeter fence; thereafter the cloud comes under the influence of the prevailing winds. For Apollo 13 the three NMIMT stations located from northeast to north-northwest of the launch pad all showed an initial positive excursion of field succeeded by a much smaller negative change; the three SRI sites situated approximately to the west-northwest of the pad gave a very similar behavior.* In the case of Apollo 13 the north cloud would be expected first to move toward the NMIMT sites and then to be driven to the southwest by the winds so as to pass almost symmetrically the center of the three SRI locations. With this cloud motion and the observed field records the straightforward interpretation is that the north cloud is bipolar in its charge structure, with positive charge in its upper portions and negative toward the base. At first the records are dominated by the field due to the positive charge, but as the cloud rises, the well-known reversal-distance effect causes the zone influenced by the negative charge to increase. Horizontal motion of the cloud will, of course, also affect the areas dominated respectively by the influence of the positive and negative charges.

For Apollo 14 all the three SRI stations to the west-northwest of the pad showed only positive field excursions; furthermore, these field changes are substantially less than those observed for Apollo 13. This behavior is consistent with the bipolar charge structure of the north cloud indicated by the Apollo 13 results, since for Apollo 14 the north cloud was always receding, first to the north and then to the east, from the three SRI sites. Consequently, these stations would always be well

---

* Although the recorders had stopped by the time of launch at two of these sites, it was possible to determine that the positive deflection preceded the negative alteration in time.

beyond the reversal distance for the north cloud, thus never experiencing negative fields, and being also sufficiently far for the positive fields not to be large. The fringes of the north cloud for Apollo 14 passed over three of the NMIMT stations--Camera Pad 1, the beach (cable) terminal, and the beach site (13.2). The records from all these stations showed negative fields. The record from 13.2 is especially interesting since it is almost a classic textbook example of the form of field variation associated with the movement of a bipolar cloud past a recording site with the closest approach being approximately equal to the reversal distance for the cloud. Initially, the field excursion is positive, to reach a maximum deviation of +500 V/m at $t \sim 30$ s; the field then declines to a minimum equal to the background level at $t \sim 60$ s; there is then an increase again to a maximum of +500 V/m at $t \sim 75$ s. The field record is asymmetric in that the minimum is not centered between the two maxima. There are many complicating factors that could account for this asymmetry. Among these are the curved trajectory, ascent of the cloud during its lateral motion, horizontal shear between charged regions of the cloud, dissipation of the charge with time by recombination, fallout, and other processes. However, a rough analysis employing the available information[15] on the cloud motion and extent indicates that the record from 13.2 is not incompatible with a north cloud containing a negative charge of the order of 10 millicoulombs (mC) in its lower region, with several tens of millicoulombs of positive charge in its upper portions.

The relative magnitudes of the upper positive charge in the north clouds for Apollo 13 and Apollo 14 can be estimated from the two respective records at Camera Pad 5 (SRI). For Apollo 14 the maximum field change ΔE of +250 V/m occurred 35 s after ignition when the north cloud had a mean height of some 300 m and was about 900 m from Camera Pad 5; if we ascribe the field change entirely to a positive charge

located at h = 300 m and r = 900 m, the corresponding charge magnitude is about 40 mC. The north cloud motion is not so well known for Apollo 13; thus the calculation is correspondingly more uncertain. However, a reasonable estimate, taking into account the cloud behavior for Apollo 14 and the different wind characteristics between the two launches, is that at Camera Pad 5, ΔE = 1200 V/m at t = 30 s, with h = 250 m and r = 400 m; it follows that the positive charge is some 24 mC. Thus it seems that the cloud electrical characteristics did not vary greatly between the two launches, the differences in the field records being largely governed by the dissimilarities in wind direction and speed.

The central cloud is of small dimensions and its effects will therefore be quite localized. For Apollo 13 the central cloud may have influenced Camera Pad 4 but the behavior at this site was almost certainly dominated by the south cloud. In the case of Apollo 14, however, the central cloud moved almost directly over Camera Pad 1 (NMIMT) and the bench terminal (NMIMT). It seems very likely that negative charge carried in the lower portions of the central cloud accounted for much of the negative field variation observed at these two NMIMT sites. Some added contribution from the lower negative charge in the postulated bipolar north cloud is also probable.

B. Radio-Noise Measurements

1. Apollo 13

Noise data obtained during the Apollo 13 launch are shown in Figure 21. Since range timing data were not recorded, it was necessary to use arguments about the recorded data to establish an absolute time base. In going over the noise record, it was observed that a marked offset in the levels of the four highest-frequency noise channels occurred shortly before the pronounced change in electric field that

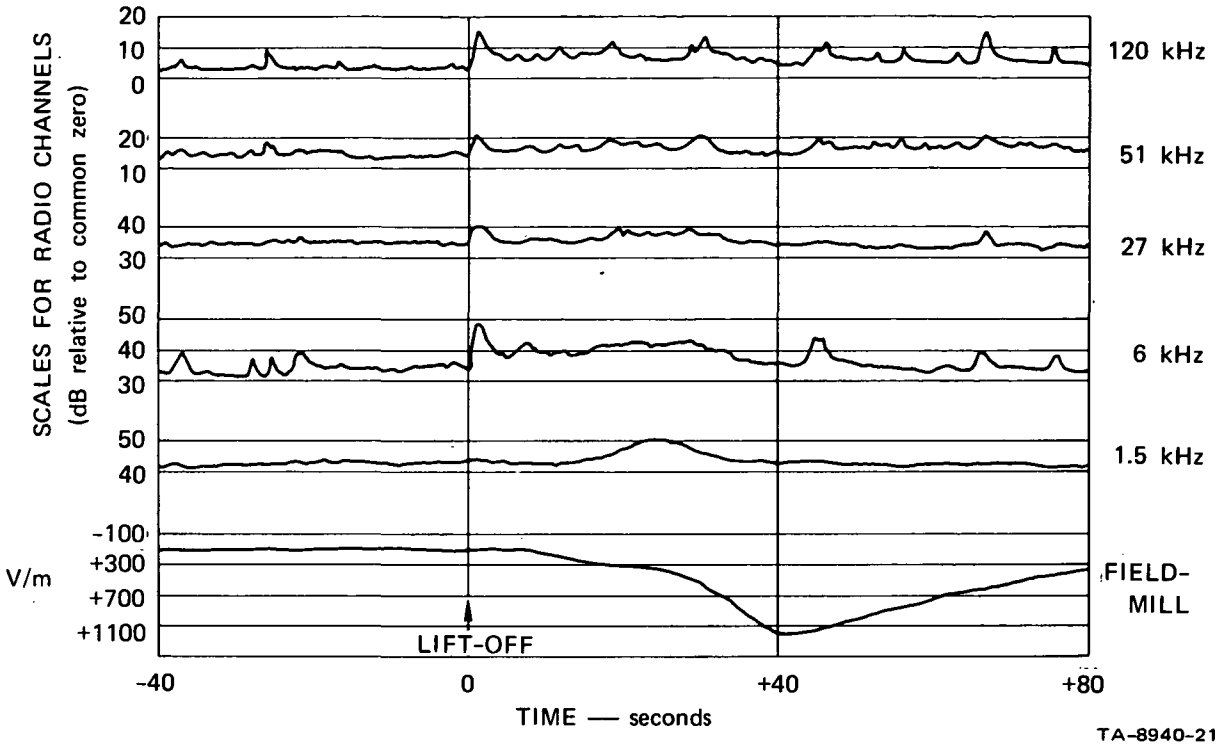

FIGURE 21 NOISE AND FIELD-METER RECORDS FROM CAMERA PAD 5 STATION DURING LAUNCH OF APOLLO 13

was associated with the launch. It was argued that this change in noise level could be associated with the charged vehicle clearing the launch pad. Accordingly, liftoff time on the record was set at the time of the noise-level change.

The results of the Apollo 13 radio-noise measurements were interesting in that they indicated that a change in the low-frequency RF noise level occurred at the general time of launch, and that the noise persisted for a period of roughly 35 s after onset. If it could be established that the trace deflections truly resulted from RF noise and not microphonics or some other spurious process in the receiving system, the noise data might provide valuable insight into the static charging of the vehicle. Some rudimentary shock tests (involving

striking various of the receiver subassemblies with a screwdriver handle) were conducted to determine if any part of the system was microphonic. No microphonics considered capable of producing the observed traces could be found. Accordingly, it was decided that the recording trace offsets were indeed caused by RF noise associated with the launch.

2. Apollo 14

To gain additional confidence in the functioning of the noise-measuring system, provisions were made on the launch of Apollo 14 to use a broadband tape recorder to record the output of the loop-antenna preamplifier. This would completely eliminate microphonics generated within the receivers by the high acoustic-noise fields associated with the launch. In addition, an electric-dipole-type antenna system was installed at the Camera Pad 5 station. This provided a completely independent source of RF noise data from receiving antenna through recorder. To provide information on vibrational noise levels, an accelerometer was installed on the loop-antenna preamplifier housing and its output was recorded on a trace of the tape recorder. Finally, timing signals were provided to both the tape recorder and the strip-chart recorder.

The RF-noise-measurement strip-chart-recorder output data obtained during the Apollo 14 launch are shown in Figure 22. These records, obtained using the loop antenna, indicate a large increase in noise on the 1.5-kHz and 5-kHz channels 3 s after ignition, while the 51-kHz channel noise does not begin until 2 s after liftoff. This behavior is quite different from that illustrated in Figure 21 where the initial change in noise level occurred simultaneously on all channels from 6 kHz through 120 kHz, and the peak of the perturbation in the 1.5-kHz noise level occurred 25 s later. To check the validity of the Apollo 14

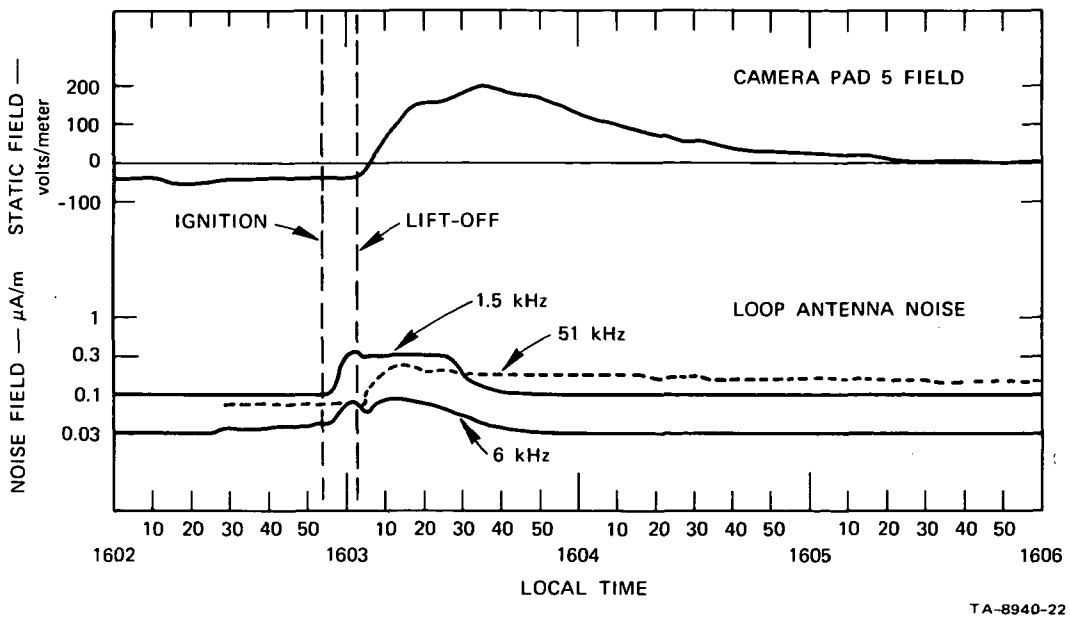

FIGURE 22 STRIP-CHART-RECORDER NOISE AND FIELD-METER RECORDS FROM APOLLO 14 LAUNCH

strip-chart noise data, the noise receivers used during the launch were set up in the laboratory; the tape-recorded broadband noise data obtained from the loop-antenna preamplifier and from the electric-dipole-antenna preamplifier during the launch were then fed into the receivers. The receiver outputs obtained during this experiment are shown in Figure 23.

It is of interest first to compare the loop-antenna data of Figure 23 with those of Figure 22. The two records display the same general signal-level variations, demonstrating that receiver microphonics did not appreciably influence the data of Figure 22. Next, it is interesting to compare the loop and electric-dipole-antenna data in Figure 23. Again, the field-intensity records are in quite good agreement. Since completely different sensors and antenna preamplifiers were used in obtaining these data, this good agreement means that preamplifier or antenna microphonics can also be discounted as having influenced the noise-field-intensity data. Thus, the RF-noise records of Figures 21, 22, and 23

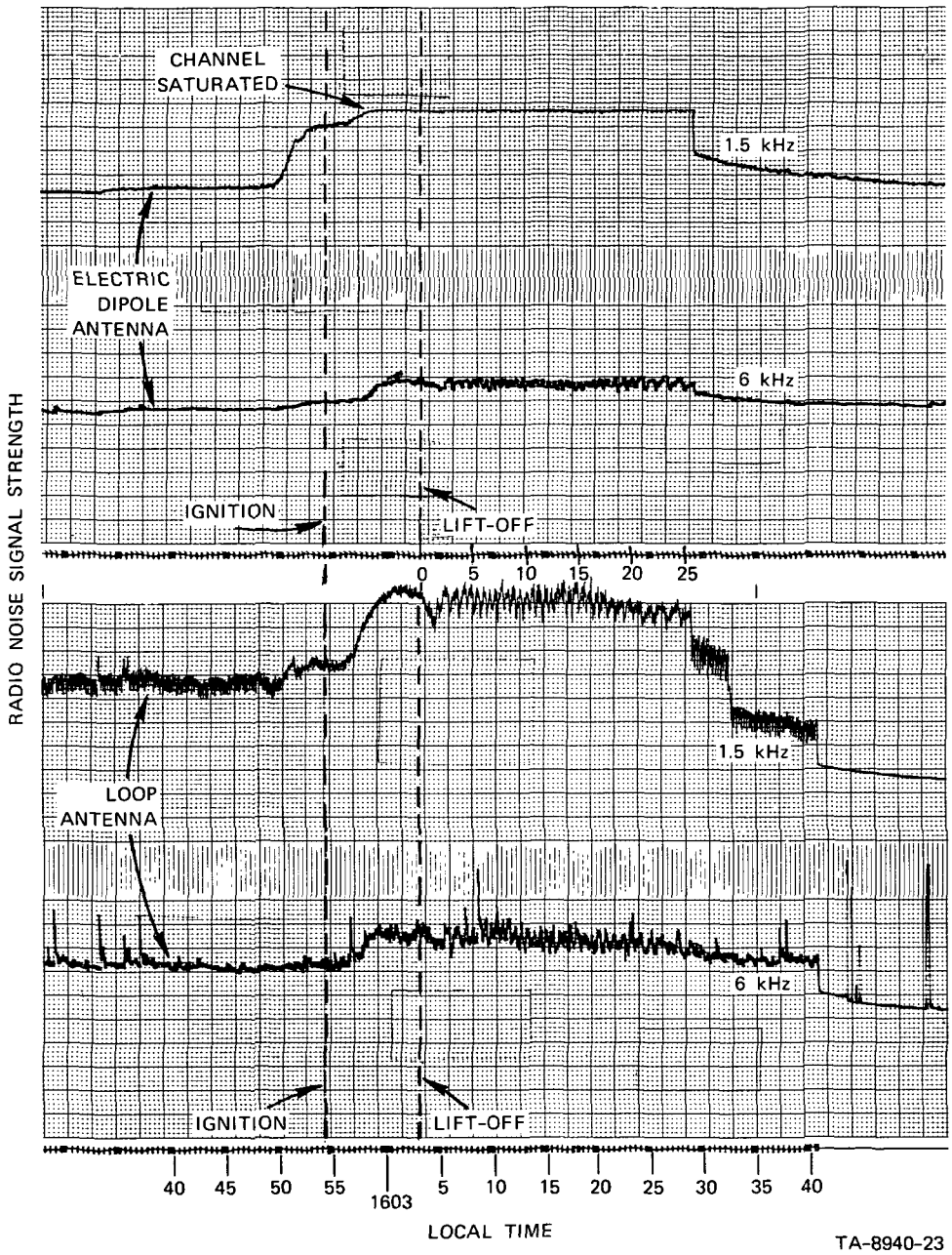

FIGURE 23 APOLLO 14 RADIO-NOISE-SIGNAL STRENGTHS FROM BROADBAND TAPE-RECORDER DATA

can be considered to be representative of the true radio-noise environment during launch.

When the data reduction had proceeded this far, it was argued that since 1.5- and 6-kHz noise starts shortly after Apollo 14 ignition, this noise might be attributed to plasma processes occurring in the exhaust. Because 51-kHz noise did not occur until after liftoff, it was felt that it might be ascribed to voltage-breakdown processes (possibly along the exhaust) associated with vehicle charging after launch. Unfortunately, the 51-kHz noise starts at 1603:05 before the rocket has cleared the LUT, when, according to LUT field-mill data, the vehicle potential is probably too low to support substantial noise-producing breakdowns from the vehicle.

In an effort to extract additional information from the RF noise records, a rayspan readout was made of the wideband tape recordings of both the loop and electric-dipole noise. The rayspan data are shown in Figure 24, in which time is plotted along the horizontal axis and frequency along the vertical axis, and noise-field intensity is proportional to the darkness of the trace. To gain an idea of the characteristics of the vibrational environment at the loop-antenna base, a rayspan readout was also made of the accelerometer signal and is shown at the bottom of Figure 24. Inspection of the figure indicates that there is a marked change in the launch-pad electromagnetic environment near the time of launch. (The record also indicates that data were not generated by microphonics, because there is no correlation between the RF noise data and the accelerometer signal.) At 1602:28 (21 s before ignition) broadband white-noise-like interference becomes evident on the electric dipole. A little later, at 1602:33 (16 s before ignition) four discrete signals appear starting at zero frequency and, in one second, sweeping up in frequency to rest at 2.5, 5, 7.5 and 10 kHz, as though some high-inertia

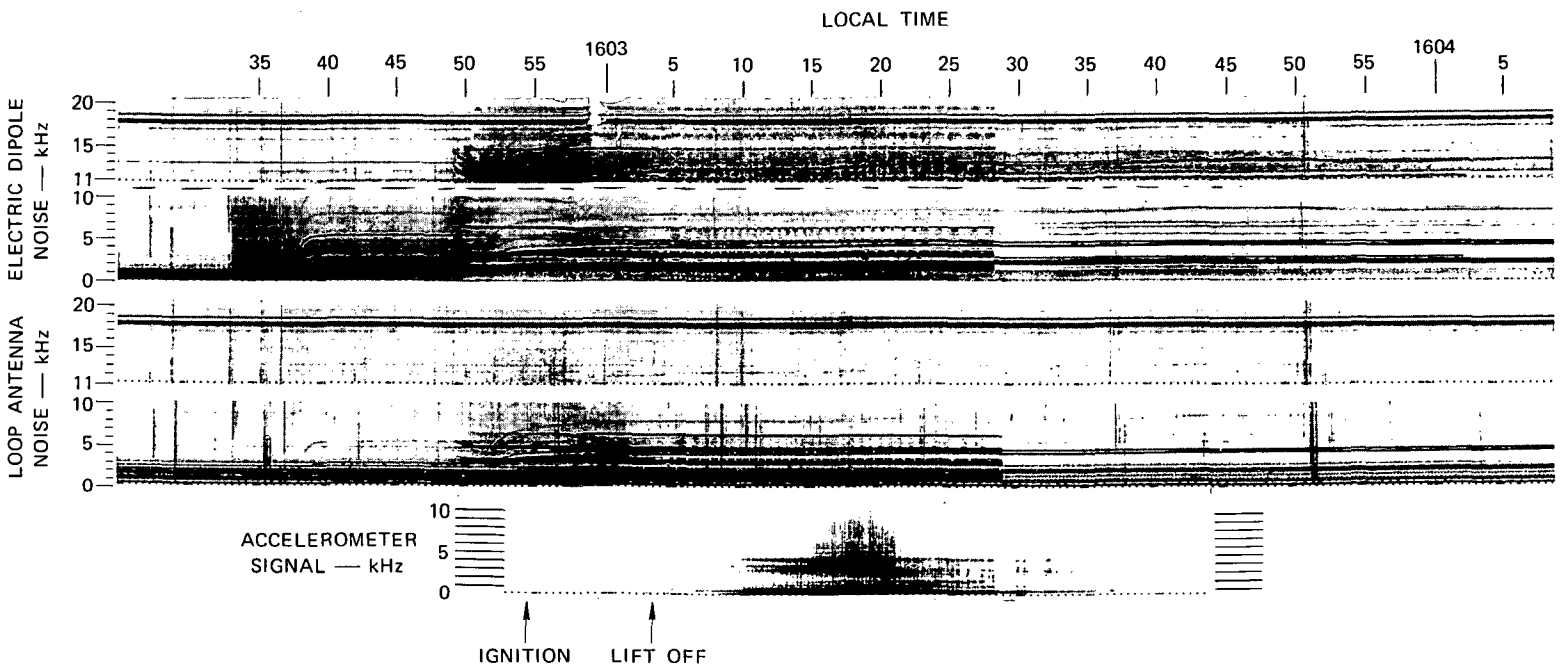

FIGURE 24 SIGNALS MEASURED DURING LAUNCH OF APOLLO 14

device such as a motor were being brought up to speed. These signals appear to stop abruptly at 1604:03. At 1602:49 (5 s before ignition) additional discrete signals appear. At 1602:51 (3 s before ignition) another group of roughly five upward-sweeping discrete signals (high inertia associated with various prelaunch activities such as turning on pumps, recorders, etc., immediately prior to launch) appear on the record.

After ignition (at 1602:57.5) some broad signals centered about discrete frequencies appear at low frequencies in Figure 24 (particularly on the loop antenna). It is apparently these latter broad signals that were responsible for the signal-strength records obtained on the 1.5- and 6-kHz noise receivers since large increases in signal strength occurred on the receiver records at roughly 1602:57.5. Some of these broad, but discrete noise signals are clearly modulated at a rate varying from 1 to 2 cps starting at 1603:05.4. This modulation is evident in Figure 23 as a series of peaks in the 1.5-kHz loop-antenna signal level starting at 1603:05.5. This same modulation is evident in the 6-kHz electric-dipole record, but not in the 1.5-kHz dipole channel which was saturated at this time. The modulated noise signals disappear abruptly at 1603:28.8 in the rayspan record of Figure 24. This corresponds to the first abrupt drop in the 1.5-kHz loop-antenna signal level, which occurs at the same time. (It should be noted that the rayspan readout has a limited dynamic range, so that had the gain of the system been increased, similar to increasing the "contrast" on a television receiver, the records would be generally darker, but might indicate that some signal persisted at 1.5 kHz after 1603:28.8 in agreement with the field-strength record of Figure 23.)

It is interesting to pursue the discussion of the last paragraph somewhat further, and to attempt to correlate the various aspects of this unusual noise signal with events associated with the launch.

First, let us look into the possible relationship between the noise record and the vehicle flight. The noise starts after ignition and changes character 2.4 s after liftoff when the vehicle is 4.25 m off the pad. It persists until almost 30 s after launch, at which time the vehicle enters the bottom of the cloud deck at 4,000 ft. Since, from Figure 23, the signal level of this noise is virtually unchanged until the rocket is at 4,000 ft altitude, it is difficult to see how a source on the rocket itself could be solely responsible for the observed signal. If the source were on the rocket, one would expect a considerable diminution in signal strength as the rocket climbed.

In casting about for other possible sources of this noise, it is noteworthy that certain of the launch-pad water systems operate over roughly the same time interval as the noise. From Figure 25 we find that during an Apollo launch, the flame-trench system B and LUT-deck

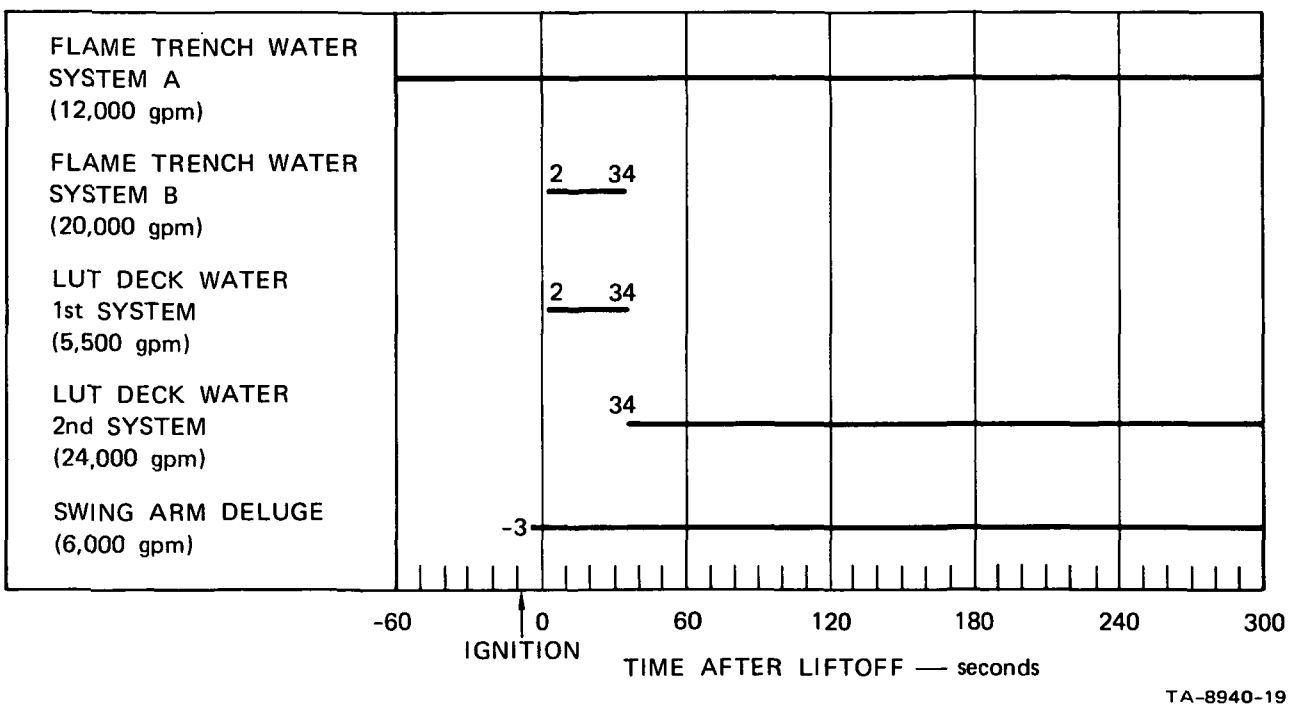

FIGURE 25 ACTIVITY OF PAD WATER-DELUGE SYSTEM DURING APOLLO LAUNCH

first system are both on from 2 s prior to liftoff until 34 s after liftoff. It is known that spraying water becomes charged, and the resulting field intensities can become sufficiently high for RF noise-producing electrical breakdowns to occur.[16] Also, the electrostatic-field measurements show conclusively that the clouds, produced by the interaction of the hot exhaust with the water and the flame trenches, are strongly charged. It is very plausible that breakdowns generating radio noise could occur within these clouds. The exact manner, however, in which these processes would operate in the high-temperature environment associated with liftoff is not obviously explained. Finally, it is peculiar why electrification and noise should be apparently associated with the operation of the water systems that function from 2 to 34 s after launch and not with others shown in Figure 25 that operate at various times from -60 to +300 s from liftoff.

IV DISCUSSION AND CONCLUSIONS

A. Vehicle Charge

In conclusion it may be stated that the Apollo 13 and 14 measurement programs were successful. Various minor difficulties did not detract appreciably from the usefulness of the data. The addition of the field meter on the LUT and the tape recorder at Camera Pad 5 for the Apollo 14 launch added most significantly to confidence in the data and its interpretation. In particular, it is now established (primarily from the LUT field-meter record) that the vehicle has relatively low charge as it leaves the LUT. This behavior is consistent with the work of Uman;[17] he has indicated that the visible plume (length approximately 200 m at ground level) is a uniformly good conductor, but that the conductivity drops quite rapidly with further increasing distance along the exhaust trail. Thus we may expect the vehicle to maintain a conducting connection with the ground at least to an altitude exceeding 200 m. Because of this conducting connection the vehicle cannot develop a substantial self-charge; the measurements show that at the time the nozzles pass the LUT the charge is only 12 μC (potential 6,000 V) or less. It is probable that the rocket potential rises abruptly once the plume clears the ground. In this regard, it would be useful to install a field meter or other equipment on one of the lower stages of a future Apollo vehicle to provide a direct measure of vehicle potential as the vehicle ascends. This experiment has been very successfully accomplished on two Titan III-C rockets,[18] and it was found that, although vehicle potential is relatively low initially after liftoff, it can achieve hundreds of kilovolts later in the flights. It is reasonable to assume similar behavior for the Apollo

vehicles, although the differences in size and engine types makes precise extrapolation difficult.

It is noteworthy that even with a potential of a million volts (a threshold value apparently of much significance in the triggering of lightning)[3] on the Apollo vehicle, the charge is only about 2 mC. Since the charges developed on the exhaust clouds are an order of magnitude greater than this it is obviously extremely difficult to deduce the electrical conditions on the vehicle from ground-level observations. Airborne measurements from balloons, rockets, or aircraft in the vicinity of the ascending vehicle are more promising, but even so there are sensitivity problems. It is difficult, for example, to reduce the noise level on a field meter mounted on an aircraft much below a few volts per meter. For a vehicle charge of 2 mC a field of 3V/m, for instance, will be exceeded only within some 3 km of the vehicle; safety constraints will often prevent such a close approach. It is significant that the aircraft measurements* during the Apollo 13 launch were reported as indicating that the vehicle charge was not greater than 3 mC; this value was probably the lower detectable limit. In order to study the vehicle electrification as already indicated, by far the most productive approach would be to install instrumentation on one of the lower stages of the launch vehicle to measure vehicle potential during the launch and subsequently.

B. Charged Exhaust Clouds

From the data obtained on Apollo 13 and 14, the launch of the rocket does not produce any large-scale shorting of the earth's field of the type that might reduce the natural fair-weather level of $\sim$ 100 V/m to almost zero. Instead, very localized field perturbations are generated associated with charge on the exhaust clouds. It should be observed, of course, that

---

*Reported at the KSC Lightning Experiments Review Meeting of January 7, 1971.

Apollo 13 and 14 were both launched under very low field conditions such that modifications in ambient field were easily masked by local charged clouds generated by the launch. The launch rules, with their emphasis on the avoidance of disturbed weather conditions associated with high electrical fields, almost ensure that future launches will be made only in a low-ambient-field environment.

It is clear that the clouds generated by the rocket exhaust and its interaction with the cooling systems are charged. However, any precise estimate of the magnitudes and distributions of the charges within the clouds cannot be made from the data provided by the field-mill network. Even for the very simple case of an intracloud lightning flash between two centers of charge it is well known that measurements from seven ground stations are required if the parameters involved are to be accurately defined. During the Apollo launches it appears that at least three charged clouds are generated; that charge generation is possible throughout the time the exhaust plume is in contact with the pad environment and perhaps later; that more than one charge-generating mechanism is involved; that some of the charged constituents fall out faster than others from the clouds; and that the position, the horizontal development, and the vertical extent of the clouds are all major influences in determining the ground electrical effects. There could well be other significant factors such as a complicated structure of the charged regions within the visible clouds, and a redistribution with time of this structure as a result of such agencies as gravitational settling, recombination, internal discharges, and corona. We may state with some confidence that the electrical structure within any individual cloud will change with time, and that the field pattern at the ground, being determined both by the positions and the internal electrical structures of the individual clouds, will show a complicated spatial and temporal variation. Under these circumstances any unique deduction, from ground

observations, of the electrical histories for each cloud, seems almost impossible.

The arguments in the preceding paragraph do not imply that no estimates can be made of the electrical characteristics of the various clouds. Rather they are intended to show that only order-of-magnitude estimates are justifiable. Such estimates are listed in Table 3. Some of the information given in Table 3 differs from that deduced by the NMIMT workers.[15] As regards the controversial points, we conclude that the north cloud is bipolar; we derive this from the negative fields observed at the SRI and NMIMT stations for Apollo 13, and from the field pattern recorded at beach Site 13.2 (NMIMT) for Apollo 14. The latter record yields the magnitude estimate for the lower negative charge. From the parking lot (SRI) record for Apollo 14, we deduce that the south cloud is bipolar. These data also enable the approximate size of the upper positive charge in the south cloud to be deduced. Our justification for postulating a bipolar structure for the central cloud is much more slender; the main arguments are that if the north and south clouds are bipolar it seems plausible that the central cloud should also have a similar structure, and that since the central cloud is so small and its electrical effects therefore very localized, nothing in the experimental data is incompatible with the postulation that it is bipolar.

Some apparently accurate estimates of the cloud charges have been deduced by the NMIMT researchers.[15] We consider these estimates to be misleadingly precise for several reasons. The estimates are based on an analysis that envisages the north cloud to be monopolar positive, the south cloud to be monopolar negative, and the central cloud to be monopolar negative; we believe that the north and south clouds at least are bipolar. The NMIMT interpretation postulates a fallout sequence from the south cloud that is speculative. Most importantly, the NMIMT analysis considers only a portion of the NMIMT data acquired during the Apollo 14 launch in the deduction of the cloud charges. The remainder of the NMIMT

data are dismissed as not fitting the deduced Apollo 14 charge distribution, while the SRI measurements made for the Apollo 14 launch and all the data (SRI and NMIMT) acquired for Apollo 13 are ignored.

Table 3

ELECTRICAL STRUCTURE OF EXHAUST-GENERATED CLOUDS AT APOLLO LAUNCHES
(Approximately 40 s After Ignition)

Cloud	Structure	Charge Upper Positive	Magnitudes Lower Negative	Remarks
North	Bipolar (Positive above, negative below)	Several tens of millicoulombs	Order of ten millicoulombs	
South	Bipolar (Positive above, negative below)	Order of ten millicoulombs	A few millicoulombs	Lower negative charge probably carried on particles that fall out rapidly
Central	Bipolar? (Positive above? Negative below.)	?	A few millicoulombs	A small cloud. Structure can only be deduced if it passes close to a recording station.

Comparisons between the behavior during the Apollo 13 and 14 launches show that in each case the upper positive charge on the north cloud was of the order of several tens of millicoulombs. During each launch also there appeared to be an early fallout of particles carrying negative charge from the south cloud. These similarities lead us to the general conclusion that there were no gross differences in the characteristics of the electrified clouds for the two launches. Nothing in the data indicates such differences.

The precise mechanisms responsible for all of the electrical effects produced on the ground are not clear. They apparently have to do with charging processes occurring in the exhaust clouds leaving the flame trench. These processes are affected by the temperature and composition of the effluent from the trench, since no electrical effects are observed until liftoff. (Apparently no charging was observed by NMIMT in the clouds generated in a static Saturn rocket firing in Mississippi in Summer 1970.[19])

Summarizing, all indications are that charge in the exhaust clouds leaving the trench does not in itself present any launch hazard. The only serious electrical incident during the Apollo launches was the lightning strike to Apollo 12 when it was at altitude in flight. There is no evidence of any adverse occurrence at ground level during any launch. Since the cloud electrification appears relatively constant for each launch the natural deduction is that the electrification is not a hazard.

Accordingly, detailed study of the electrical structure of the exhaust clouds is likely to be more basic than applied in its impact. The controlled nature of the launch procedures, and the apparent reproducibility of the electrical effects, suggest a fruitful area of experimental research for the academic scientist interested in the sudden and massive occurrence of exotic charging mechanisms.

C. Radio Noise

The purpose of the RF noise measurements, carried out during the launches of Apollo 13 and 14, was to take advantage of the fact that RF noise-producing electrical discharges occur from a highly charged vehicle, in an effort to get an indication of rocket potential shortly after liftoff. Changes in the RF noise level were observed on both

launches. Noise-signal-strength records on the two launches were different, leading to the initial conclusion that the noise was caused by processes associated with vehicle flight, and not by radio-frequency interference associated with the launch complex; this interference one would expect to be relatively the same from launch to launch. Following a more careful analysis of the Apollo 14 noise data including a rayspan readout (in which the spectral history of the noise is displayed) it became clear that, for Apollo 14 at least, much of the RF noise occurring near the time of launch, although associated with launch processes, was not generated on the vehicle itself. This is clearly indicated by the fact that the noise persisted with undiminished amplitude until the vehicle altitude was 4000 ft; this fact is quite inconsistent with a noise source on the vehicle.

Some effort was made to correlate the noise with other launch-associated activities occurring on the pad such as the water-deluge-system operation and the consequent generation of charged clouds. Here the time correlation with operation of Flame Trench B and LUT Deck No. 1 systems appears reasonable. Unfortunately, again, there were other similar water systems operating at times when the noise in question did not exist. It may be that only some of the water systems create charged clouds, but this point is difficult to establish.

In conclusion, it appears on the basis of the meager Apollo 13 RF noise data and the more substantial Apollo 14 data, that in the frequency range studied, the RFI generated near the time of launch by various activities associated with the launch substantially masks any RF noise that might be generated by electrification of the vehicle itself. Thus, using ground-level data obtained at discrete frequencies on a single launch to infer the electrostatic behavior of the rocket is not likely to be successful. If, however, broadband RF noise measurements are made

at spaced locations on several launches and on their respective countdown demonstration tests, it might be possible to obtain some useful information in this way. An unexpected dividend of such a network of measurements might be an identification of noise sources with particular clouds; this would be an indicator of their degree of electrification.

V RECOMMENDATIONS

The following are the recommendations that emerged from this study:

(1) The existing launch rules regarding launching during disturbed weather should not be relaxed at this time. Intrusion of a body the size of the Apollo vehicle is likely to trigger a lightning stroke in a region of high electric field. The results of the present program confirm that the electrical length of the vehicle is increased by the highly conducting rocket exhaust.

(2) We think it vital that, since the charged clouds generated by the launch obscure the other electrical effects produced by the launch, consideration should be given to the installation of a field meter on one of the lower stages of a future Apollo vehicle. This instrument would provide unequivocal information on the vehicle charge irrespective of charged clouds near the ground. It would also show whether or not substantial charges develop on the vehicle after it becomes removed from the immediate vicinity of the launch pad. This measurement is most important because there is strong evidence that the presence of a potential approaching a million volts (2 mC charge on an Apollo vehicle) on a conductor is one of the two necessary criteria for the occurrence of a lightning-initiating streamer from the conductor.[3] It is difficult to see how such a potential could be reliably detected except by an instrument carried on the vehicle.

(3) We believe it desirable that in order to further define the electrical character of the launch vehicle and the way in which it perturbs the ambient fields, tests of the sort conducted on Apollos 13 and 14 should be continued. A fixed array of ground field meters should be located around the pad, and in particular, the LUT field meter should become a permanent installation. These measurements are necessary to develop confidence

in the data obtained to date, and to look for deviations from the behavior observed thus far. Variations observed in the readings at the same location on Apollos 13 and 14 (depending on wind direction) indicate that the array of field meters should continue to surround the pad. If the array of field meters becomes a permanent installation, it is also available to supply real-time data on the degree of disturbance of the natural atmospheric electrical environment; these data can be used as a supplemental input in the making of launch-delay decisions.

REFERENCES

1. R. Godfrey, "Analysis of Apollo 12 Lightning Incident," MSC-01540, Marshall Space Flight Center, Kennedy Space Center (February 1970).

2. E. T. Pierce, "Lightning Discharges to Tall Structures," EOS, Vol. 51(4), p. 301 (April 1970).

3. E. T. Pierce, "Triggered Lightning and Some Unexpected Lightning Hazards," Scientific Note 15, SRI Project 4454, Contract N00014-71-C-0106, Stanford Research Institute, Menlo Park, Calif. (January 1972).

4. J. E. Nanevicz, E. T. Pierce, and A. L. Whitson, "A Preliminary Report on Atmospheric Electricity Measurements During the Launch of Apollo 13," Consultant Report, SRI Project 8553, Contract P.O. 1-90298, Stanford Research Institute, Menlo Park, Calif. (April 1970).

5. E. T. Pierce and J. E. Nanevicz, "Preliminary Report on SRI Apollo 14 Experiment," Consultant Report, SRI Project 8940, Contract NAS9-11357, Stanford Research Institute, Menlo Park, Calif. (March 1971).

6. R. L. Tanner and J. E. Nanevicz, "Precipitation Charging and Corona-Generated Interference in Aircraft," Technical Report 73, Contract AF 19(604)-3458, Stanford Research Institute, Menlo Park, Calif. (April 1961).

7. R. L. Tanner and J. E. Nanevicz, "Radio Noise Generated on Aircraft Surfaces," Final Report, Contract AF 33(616)-2761, Stanford Research Institute, Menlo Park, Calif. (September 1956).

8. E. F. Vance and J. E. Nanevicz, "Rocket Motor Charging Experiments," Scientific Report 2, SRI Project 5359, Contract AF 19(628)-4800, Stanford Research Institute, Menlo Park, Calif. (June 1966).

9. E. T. Pierce, "Perturbations Produced by Jet Aircraft in the Earth's Electric Field," J. Appl. Meteor., Vol. 3, pp. 805-806 (1964).

10. M. Brook and C. B. Moore, "Atmospheric Measurements of the Launch of Apollo 13," Preliminary Report, New Mexico Institute of Mining and Technology, Socorro, N.M. (11 April 1970).

11. J. E. Nanevicz, "Progress in the Study of the Titan Vehicle Electrostatic Environment," Engineering Data Design Evaluation Report, SRI Project 8428, Contract F33615-70-C-1406, Stanford Research Institute, Menlo Park, Calif. (May 1971).

12. J. A. Stratton, Electromagnetic Theory, p. 209 (McGraw Hill Book Co., Inc., New York, N.Y., 1941).

13. M. Brook, C. R. Holme, and C. B. Moore "Lightning Rockets: Some Implications of the Apollo 12 Lightning Incident," Naval Research Review, Vol. 23(4), pp. 1-17 (April 1970).

14. W. R. Smythe, Static and Dynamic Electricity (McGraw Hill Book Co., Inc., New York, N.Y., 1950).

15. M. Brook and C. B. Moore, "Report on Atmospheric Electric Measurements During the Launch of Apollo 14," New Mexico Institute of Mining and Technology, Socorro, N.M. (May 1971).

16. E. T. Pierce, "Waterfalls, Bathrooms, and Perhaps Supertanker Explosions," Proc. 1970 Lightning and Static Electricity Conference, 9-11 December 1970, sponsored by Society of Automotive Engineers and Air Force Avionics Laboratory, San Diego, Calif.

17. M. A. Uman, "Electrical Breakdown in the Apollo 12/Saturn V First Stage Exhaust," Report 70-9C8-HIVOL-R1, Westinghouse Research Laboratories, Pittsburgh, Pa. (1970).

18. J. E. Nanevicz, et al., "Titan Vehicle Electrostatic Environment," Final Report, SRI Project 8428, Contract F33615-70-C-1406, Stanford Research Institute, Menlo Park, Calif. (in preparation).

19. Private communication.